
SEEQUENT
Heat and Mass Transfer Modeling with GeoStudio
GeoStudio

Email: sales@geoslope.com

Contents

Symbols

α Albedo

α Dispersivity of soil/medium, m
- in longitudinal direction, α_L
  - in air phase, α_{La}
  - in water phase, α_{Lw}
- in transverse direction, α_T
  - in air phase, α_{Ta}
  - in water phase, α_{Tw}

α Apparent dip angle, °

α Slope angle for surface mass balance

α_{rw} Root water extraction reduction factor

α_w Volumetric coefficient of thermal expansion at constant pressure, /K

β Soil structure compressibility, /kPa

β_w Isothermal compressibility of water, 4.8×10^{-10} /kPa at 10 °C

β' Angle between the dip direction and the apparent dip direction, °

γ Psychrometric constant, 0.0665 kPa/C

γ Dip direction, °

Γ Slope of the saturation vapor pressure vs. temperature curve, kPa/C

δ Solar declination, radians

δ Dip angle, °

Δt Time increment

Δx Nodal spacing

ε Emissivity
- air emissivity, ε_a

η Dynamic viscosity, kg/s/m

θ Normalized time for sinusoidal radiation distribution, radians

θ Volumetric content, m^3/m^3
- water content, θ_w
- unfrozen water content, θ_{uwc}
  - at a given temperature, θ'_{uwc}
- saturated water content, θ_{sat}
- residual water content, θ_{res}
- lower limit of the volumetric water content function, θ_L
- air content, θ_a
- ice content, θ_{ice}

θ_{eq} Equivalent diffusion porosity, m^3/m^3

λ Decay constant, /s

ν Poisson's ratio

ρ Mass density, g/ m^3
- soil dry bulk density, ρ_d
- of air, ρ_a
- of water, ρ_w
- of solids particles, ρ_s
- of snow, ρ_{snow}
- of ice, ρ_{ice}

σ Stefan-Boltzmann constant, 5.67×10^{-8} $W/m^2/K^4$

τ Tortuosity factor

Ψ Atmospheric stability correction factor
- for heat flux, Ψ_h
- for momentum flux, Ψ_m

φ Latitude, radians

φ Matric suction, kPa

ω_s Sunset hour angle, radians

π_{root} Root length density, m/m^3

π'_{root} Normalized water uptake distribution, /L

A Area, m^2

A Normalized amplitude for sinusoidal radiation distribution, $MJ/hr/m^2$

AE Actual evapotranspiration, $m^3/s/m^2$

A, B, n Empirical relationship constants for thermosyphon heat transfer conductance

a_s, b_s Angstrom formula regression constants

a, a', n, m Curve fitting parameters for van Genuchten (1980), Fredlund and Xing (1994) volumetric water content functions

C Courant dimensionless number

C Mass concentration, kg/m^3
- in the gas phase, C_{gp}
- of gas in the dissolved phase, C_{ap}

$C(\varphi)$ Correlation function for Fredlund-Xing (1994) volumetric water content function

$C^{(m)}$ FEM constitutive matrix

C_p Volumetric heat capacity, $J/m^3/K$
- of liquid water, C_w
- of vapor, C_v
- of air, C_a
- of solids, C_s
- of ice, C_{ice}
- of soil at a given water content, C'_p
- of a partially frozen soil, C_{pf}
- apparent volumetric heat capacity, C_{ap}

c_p Specific heat capacity, J/kg/K
- of liquid water, c_w
- of vapor, c_v
- of air, c_a
- of solids, c_s
- of moist air, c_{sa}

D Coefficient of diffusion or dispersion, m^2/s
- diffusion of water vapor in soil, D_v
- bulk mass diffusion coefficient, D_d^*
- bulk diffusion coefficient for gas phase, D_{da}^*
- bulk diffusion coefficient for gas

	in dissolved phase, D_{dw}^{*}
	mechanical dispersion, D'
	hydrodynamic dispersion, D
	hydrodynamic dispersion of gas in gas phase, D_a
	hydrodynamic dispersion of gas in dissolved phase, D_w
D	Diameter, m
	10% passing on grain size curve, D_{10}
	60% passing on grain size curve, D_{60}
D_{vap}	Diffusivity of water vapor in air at given temperature, m^2/s
d	Zero-displacement height of wind profiles, m
d_r	Inverse relative distance from Earth to Sun, m
E	Modulus of elasticity
E	Long-wave radiation, MJ/m^2/day
E_a	Aridity
E_b	Maximum emissive power of an ideal radiator
$\dot{E}$	Rate of energy change, W
	transfer into control volume, $\dot{E}_{in}$
	transfer out of control volume, $\dot{E}_{out}$
	generated in control volume, $\dot{E}_g$
	stored in a control volume, $\dot{E}_{st}$
$f(u)$	Latent heat transfer coefficient as a function of wind speed, MJ/m^2/kPa/day
G_{SC}	Solar constant, 118 MJ/m^2/day
g	Gravitational constant, m/s^2
H	Dimensionless Henry's equilibrium constant
h	Convection heat transfer coefficient, W/m^2/K
h	Relative humidity
	of the soil, h_s
	of the air, h_a
	daily maximum (air), h_{max}
	daily minimum (air), h_{min}
h	Depth / height, m
	of a crop, h_c
	of precipitation, h_P
	of snow, h_{snow}
	incremental snow accumulation, Δh_{snow}
	incremental snowmelt depth, Δh_{melt}
	incremental snow-water equivalent accumulation, Δh_{swe}
h_i	Finite element interpolating function for the primary variable
h_{fg}	Latent heat of fusion, J/kg
h_{sf}	Latent heat of vaporization, J/kg
I	Freeze/thaw index, K-days
	of the air, I_a
	of the ground surface, I_g
J	Mass flux, kg/s/m^2
	associated with dispersion, J_D
	associated with advection, J_A
	total surface mass flux at free exit boundary, J_s
J	Day of the year
K	Bulk modulus, N/m^2
K	Hydraulic conductivity, m/s
	of isothermal liquid water, K_w
	of a fluid, K_f
	of dry air, K_a
	of an unfrozen soil, K_u
	of a frozen soil, K_f
	of a partially frozen soil, K_{pf}
	of a saturated soil, K_{sat}
	of a dry soil, K_{dry}
	of soil at a given water content, K'
	in the x direction, K_x
	in the y direction, K_y
	in the z direction, K_z
$K_{x'}/K_{x'}$	Hydraulic conductivity anisotropy ratio
$K_{z'}/K_{x'}$	Hydraulic conductivity anisotropy ratio
K_d	Adsorption coefficient
K_r^*	Bulk reaction rate coefficient for irreversible first order reactions, 1/s
$K^{(m)}$	Element characteristic matrix for FEM
k	Canopy radiation extinction constant
k	Von Karman's constant, 0.41
k	Thermal conductivity, W/m/K
	of soil solids, k_s
	of liquid water, k_w
	of a fluid, k_f
	of snow, k_{snow}
	of an unfrozen soil, k_u
	of a frozen soil, k_f
	of a saturated soil, k_{sat}
	of a dry soil, k_{dry}
L	Characteristic length, m
LAI	Leaf area index
M	Molar mass, kg/mol
M	Mass, kg
	of water vapor, M_v
	of liquid water, M_w
	of solids, M_s
MF	Thermal conductivity modifier factor
MF	Snow depth multiplier factor
$M^{(m)}$	FEM element mass matrix

$\dot{M}$ Stored mass rate of change, kg/s
- of all water stored in REV, $\dot{M}_{st}$
- of liquid water stored in REV, $\dot{M}_w$
- of all air stored in an REV, $\dot{M}_g$
- of water vapor stored in REV, $\dot{M}_v$
- of dry air stored in REV, $\dot{M}_a$
- of dissolved dry air stored in REV, $\dot{M}_d$
- of adsorbed mass phase in REV, $\dot{M}_{ap}$
- of dissolved mass phase in REV, $\dot{M}_{dp}$
- of mass added to REV, $\dot{M}_S$
- due to decay reactions, $\dot{M}_\lambda$

$\dot{m}$ Mass rate of change due to flow, kg/s
- flow into a control volume, $\dot{m}_{in}$
- flow out of a control volume, $\dot{m}_{out}$
- flow of liquid water, $\dot{m}_w$
- flow of water vapor, $\dot{m}_v$
- flow of air, $\dot{m}_a$
- due to diffusion, $\dot{m}_D$
- due to advection, $\dot{m}_A$
- perpendicular to control surfaces of x, y and z coordinates, $\dot{m}_x, \dot{m}_y, \dot{m}_z$

m_w Slope of the volumetric water content function, m^2/N

m_v Coefficient of volume change, /kPa

N Maximum possible duration of sunshine or daylight, hours

Nu Nusselt dimensionless number

n Porosity

n Actual duration of sunlight, hours

n n-Factor

Pe Péclet dimensionless number

p_v Vapor pressure, kPa
- of air above the soil, p_v^a
- of saturated air, p_{v0}^a
- at the soil surface, p_v^s
- at the surface of a saturated soil, p_{v0}^s

$\dot{Q}$ Heat transfer rate due to conduction, J/s
- perpendicular to control surfaces of x, y and z coordinates, $\dot{Q}_x, \dot{Q}_y, \dot{Q}_z$

q Curve fitting parameter for air conductivity function, 2.9

q Volumetric flux, $m^3/s/m^2$
- of air, q_a
- of liquid water, q_w
- of fluid normal to free surface, q_n
- associated with rainfall, q_P
- associated with snow melt, q_M
- associated with infiltration, q_I
- associated with runoff, q_R
- through plant roots, q_{root}
- associated with evaporation, q_E
- of potential evaporation, q_{PE}
- of actual evaporation, q_{AE}
- of potential transpiration, q_{PT}
- of actual transpiration, q_{PT}
- of potential evapotranspiration due to radiation or aerodynamics, q_{PET}
- of user-defined daily potential evapotranspiration, $\overline{q_{PET}}$

q Heat flux, $MJ/m^2/day$
- ground heat flux, q_g
- heat flux through snow, q_{snow}
- latent heat flux, q_{lat}
- sensible heat flux, q_{sens}
- surface convective heat flux, q_{sur}
- extraterrestrial radiation, q_{ext}
- shortwave radiation, q_s
- net radiation, q_n
- net longwave radiation, q_{nl}
- net shortwave, q_{ns}

q_n^* Net radiation in terms of water flux, mm/day

q_{root}^{max} Maximum potential root water extraction rate per soil volume, $m^3/s/m^3$

R Gas constant, 8.314472 J/K/mol

Re Reynolds dimensionless number

R_i Richardson number

$R^{(m)}$ FEM nodal load vector or forcing vector

r Resistance, s/m
- aerodynamic resistance to heat flow from soil surface to atmosphere, r_a
- neutral aerodynamic resistance, r_{aa}
- bulk surface resistance, r_c
- bulk stomatal resistance of well-illuminated leaf, r_l

r_{max} Total root length, m

S Degree of saturation

S Solubility coefficient

S^* Mass sorbed per mass of solids

Sc Schmidt dimensionless number

SCF Soil cover fraction

T Temperature, K
- of air, T_a
- daily maximum (air), T_{max}
- daily minimum (air), T_{min}
- of the ground surface, T_g
- at the snow surface, T_{snow}
- of fluid at the bounding surface, T_{sur}
- of fluid outside the thermal boundary layer surface, T_∞
- normal freezing point of water at atmospheric pressure, T_0

t Time, s

	of sunrise, $t_{sunrise}$
t	Duration, days
	of the air freeze/thaw season, t_a
	of the ground surface freeze/thaw season, t_g
$t_{1/2}$	Decay half-life, s
$\dot{U}$	Rate of latent or sensible energy change, J/s
	of latent energy, $\dot{U}_{lat}$
	of latent energy from fusion, $\dot{U}_{sf}$
	latent energy from vaporization, $\dot{U}_{sf}$
	of sensible thermal energy, $\dot{U}_{sens}$
$U^{(m)}$	FEM matrix of nodal unknowns
u	Primary variable anywhere within a finite element
	at nodal points, u_i
u	Wind speed, m/s
u	Pressure, kPa
	of pore water, u_w
	of pore air, u_a
	gauge air pressure at given elevation, u_{a_y}
	absolute air pressure, $\overline{u_a}$
	reference absolute air pressure, $\overline{u_{a_0}}$
u_t	Sensible thermal energy per unit mass, J/kg
V	Volume, m^3
	of air, V_a
	total volume, V_t
VF	View factor accounting for angle of incidence and shadowing
v	Velocity, m/s
	of water, v_w
	of air, v_a
v_w	Specific volume of water, m^3/kg
y_{ref}	Reference elevation, m
z	Surface roughness height, m
	for heat flux, z_h
	for momentum flux, z_m
z_{ref}	Reference measurement height, 1.5 m

Preface

GeoStudio is an integrated, multi-physics, multi-dimensional, platform of numerical analysis tools for geo-engineers and earth scientists. The multi-disciplinary nature of GeoStudio is reflected in its range of products: four finite element flow products (heat and mass transfer); two finite element stress-strain products; and a slope stability product that employs limit equilibrium and stress based strategies for calculating margins of safety. The focus of this book is on the heat and mass transfer products.

Countless textbooks provide a thorough treatment of the finite element method and its implementation, both in a general and subject-specific manner. Similarly, there are numerous comprehensive presentations of the physics associated with heat and mass transfer in multiple disciplines, such as soil physics, hydrogeology, and geo-environmental engineering. Journal articles and conference papers abound on specific aspects of a physical processes, characterization of constitutive behaviours, and numerical strategies for coping with material non-linearity.

It follows, then, that the idea of writing a book on heat and mass transfer finite element modelling with GeoStudio is not only daunting, but also a bit presumptuous, given the breadth of material already available to the reader. Nonetheless, we feel that a review of the foundational principles associated with both the physics and the numerical approaches used by GeoStudio will have value to the reader and will assist in the effective use of the models.

It is important to note that the purpose of this 'book' is not to provide detailed instructions for operating the software. The primary vehicle for that information is the learning section for GeoStudio on the Seequent website (www.seequent.com), where the user can access example files, tutorial movies, technical webinars and our online learning platform. In addition, help topics are available during operation of the software in the Help menu (accessed by pressing F1). These resources provide valuable information for those learning how to use GeoStudio.

The first two sections of this book include a general overview of GeoStudio and the finite element method as applied to field problems. Sections 3 through 6 summarize the theoretical formulations of each flow product and provide information on the product-specific material models and boundary conditions. The ultimate objective of these sections is to help the reader understand the fundamental components of each product. Readers can gain a deeper understanding of particular topic areas by exploring the wealth of resources available in the public domain, which are referenced throughout. Appendix I includes a detailed description of the FEM solution used in GeoStudio and Appendix II provides a general discourse on the best practice for numerical modelling.

1 GeoStudio Overview

GeoStudio comprises several products (Table 1). The first four products listed in Table 1 simulate the flow of energy or mass while the following three products are used to simulate a wide range of soil mechanical behavior. Integration of many of the products within GeoStudio provides a single platform for analyzing a wide range of geotechnical and geoscience problems.

Table 1. Summary of GeoStudio applications.

Product	Simulation Objective
TEMP/W & TEMP3D	Heat (thermal energy) transfer through porous media
SEEP/W & SEEP3D	Water (Liquid water and vapor) transfer through saturated and unsaturated porous media
CTRAN/W & CTRAN3D	Solute or gas transfer by advection and diffusion
AIR/W & AIR3D	Air transfer in response to pressure gradients
SIGMA/W	Static stress-strain response and stability of geotechnical structures
QUAKE/W	Dynamic stress-strain response of geotechnical structures
SLOPE/W & SLOPE3D	Static or pseudo-dynamic slope stability using limit equilibrium or stress-based methods

Many physical processes are coupled; that is, a change in the state variable governing one process alters the state variable governing another. For example, time-dependent deformation of a soil in response to an applied load represents a two-way, coupled process. During consolidation, the rate of water flow controls the dissipation of excess pore-water pressures and causes deformation, while the generation of excess pore-water pressures is linked to the resistance of the soil skeleton to deformation. Thus, the water transfer and equilibrium equations must be solved in a coupled manner using the SIGMA/W coupled consolidation formulation.

Water and air flow through porous media provides another example of a coupled process. The flow of water and air flow depend on their respective fluid pressures while the storage of water and air depend on the differential pressure between these two phases. A similar coupling occurs during the simulation of density dependent water flow. The simulation of heat (TEMP/W) or mass transport (CTRAN/W) can utilize water flows generated in a seepage analysis (SEEP/W); however, the water flow, in turn, can be affected by variations in water density created by the distribution of heat or mass within the domain. The same type of coupling also occurs in a density-dependent air flow analysis (i.e., AIR/W and TEMP/W). Table 2 summarizes some of the processes that can be coupled in GeoStudio. Additional coupling can also be simulated using the Add-in functionality within GeoStudio. One example of this includes the use of oxygen transport and consumption within a waste rock dump (CTRAN/W) to create heating (TEMP/W), which then results in air flow (AIR/W) that drives oxygen transport (CTRAN/W).

A single GeoStudio Project file (*.GSZ) can contain multiple geometries and multiple analyses. Each analysis may contain a single set of physics (i.e., one product) or may integrate more than one set of

physics (i.e., multiple products) with various levels of dependency (i.e., coupled or uncoupled analyses). For certain scenarios involving one-way coupling, it is often convenient to simulate the independent process in a separate analysis and direct the subsequent dependent analysis to the results from the independent analysis. For example, a CTRAN/W analysis could refer to water contents and water flow rates from an independent SEEP/W analysis. This simple method of product integration is the same functionality that allows a SLOPE/W or SIGMA/W analysis, for example, to obtain pore-water pressure information from a SEEP/W analysis. However, for two-way coupling, the coupled sets of physics must be contained within a single analysis.

Table 2. Summary of the coupled heat and mass transfer formulations.

Product	Coupled Processes
SEEP/W AIR/W	Coupled water and air transfer for modelling the effect of air pressure changes on water transfer and vice versa
SEEP/W TEMP/W	Forced convection of heat with water and/or vapor transfer, free convection of liquid water caused by thermally-induced density variations, and thermally-driven vapor transfer
AIR/W TEMP/W	Forced convection of heat with air transfer and free convection of air caused by thermally-induced density variations
CTRAN/W SEEP/W	Advection of dissolved solutes with water transfer and free convection of liquid water caused by density variations due to dissolved solutes
CTRAN/W AIR/W	Advection of gaseous solutes with air transfer and free convection of air caused by density variations due to differential gas pressures
SIGMA/W	Coupled water transfer and stress-strain behavior to simulate the transient pore-water pressure and deformation response (i.e. consolidation) due to loading and/or unloading and/or changes in hydraulic conditions.

The various analyses within a project file are organized in an Analysis Tree, as illustrated in many of the example files. The Analysis Tree provides a visual structure of the analyses and identifies the 'Parent-Child' relationships. For example, a CTRAN/W analysis might be the child of a SEEP/W analysis and, consequently, the integration and dependency relationships are visible in the parent-child Analysis Tree structure. The Analysis Tree also encourages the user to adopt a workflow pattern that is consistent with the modelling methodology advocated for GeoStudio (Appendix II).

The heat and mass transfer products support one-dimensional, two-dimensional, three-dimensional (SEEP3D), plan view, and axisymmetric analysis. The formulation and finite element procedures are the same regardless of dimensionality. The selected dimensionality is incorporated during assembly of the element characteristic matrices and mass matrices (Section I.4). Assembly of these matrices involves numerical integration over the volume of the element, which requires the area and out-of-plane thickness for elements that are not three-dimensional. For a conventional two-dimensional analysis, the element thickness defaults to a unit length (1.0). The element thickness and width for a one-dimensional analysis are implicitly one unit length. A cylindrical coordinate system is adopted for axisymmetric analyses, with the conventional x axis representing a radial dimension, r. The thickness of the domain at

any point in space is the arc length, which is calculated from the specified central angle and radius r. The element thickness for a plan view analysis is the vertical distance between the upper and lower surfaces.

2 Finite Element Approach for Field Problems

The finite element method (FEM) is a numerical approach to solving boundary value problems, or field problems, in which the field variables are dependent variables associated with the governing partial differential equation (PDE). The PDE provides a mathematical description of the physical process and is generally derived by applying a statement of conservation (i.e., of mass or energy) to a representative elementary volume (REV). The REV is a control volume of finite dimensions (dx, dy, dz) representing the smallest volume of the domain for which characteristic material properties can be defined. The conservation statement relates a mathematical description of the change in 'storage' (of heat or mass) within the REV, to a mathematical description of the 'flow' processes (heat or mass transport) into or out of the REV.

These problems are considered 'field' problems because the solution is the distribution of the energy 'field' controlling flow throughout the domain of interest. In geotechnical or earth sciences, the domain is some specified volume of geologic material with known properties. The final solution is the value of the dependent variable as a function of space (and time in the case of a transient problem). The solution is constrained by boundary conditions specified over the domain boundaries. These boundary conditions follow three general forms: (1) a specified value of the dependent variable (i.e., a 1st type boundary condition); (2) the spatial derivative of the dependent variable (i.e., a 2nd type boundary condition); or (3) a secondary variable which is a function of the dependent variable (e.g., a mass or energy flux).

The numerical solution is based on the principle of discretization, in which the domain is represented by a series of 'finite elements'. Shape functions specify the distribution of the dependent variable across each of these elements. Consequently, the value of the dependent variable anywhere within the element is a function of the dependent variable at the element nodes. This discretization enables the representation of the PDE in a semi-continuous way across the entire domain, and results in a series of simultaneous equations, solved using linear algebra.

The key components of the FEM are:

1. Discretization of the domain into finite elements;
2. Selection of a function to describe how the primary variable varies within an element;
3. Definition of the governing partial differential equation (PDE);
4. Derivation of linear equations that satisfy the PDE within each element (element equations);
5. Assembly of the element equations into a global set of equations, modified for boundary conditions; and,
6. Solution of the global equations.

Appendix I provides a detailed description of the FEM. The following sections highlight three key FEM components for each product type: (1) development of the PDE describing the relevant physics; (2) the material models used to describe material behavior; and (3) the boundary conditions used to constrain the FEM solution.

3 Water Transfer

SEEP/W (or SEEP3D) simulates the movement of liquid water or water vapor through saturated and unsaturated porous media. This might include simulations of steady or transient groundwater flow within natural flow systems subject to climatic boundary conditions, pore pressures around engineered earth structures during dewatering, or the impact of flooding on the time-dependent pore pressures within a flood control dyke. In some cases, it is important to simulate both liquid and vapor water movement. An important example in this regard is the simulation of soil-vegetation-atmosphere-transfers, such as evaporation, transpiration, and infiltration in the design of reclamation soil covers for mine waste or landfills. The following sections summarize the governing physics, material properties, and boundary conditions that are foundational to a seepage analysis: Section 3.1 summarizes the water transfer and storage processes included in the formulation; Section 3.2 describes the constitutive models used to characterize water transfer and storage; and Section 3.2.4 describes the boundary conditions unique to this product. One final section provides additional information on dealing with material non-linearity and the associated challenges faced by the convergence schemes required to solve these types of problems. The symbols section at the beginning of this document has a full listing of the parameter definitions used in the following sections.

3.1 Theory

Domenico and Schwartz (1998) provide a comprehensive theoretical review of groundwater flow through porous media. The conservation of mass statement requires that the difference in the rate of mass flow into and out of the REV must be equal to the rate of change in mass within the REV, as follows:

$$\dot{M}_{st} \equiv \frac{dM_{st}}{dt} = \dot{m}_{in} - \dot{m}_{out} + \dot{M}_S \qquad \text{Equation 1}$$

where M_{st} is the stored mass, the inflow and outflow terms, m_{in} and m_{out}, represent the mass transported across the REV surface, and M_S represents a mass source or sink within the REV. The over-dot indicates a time-derivative (rate) of these quantities.

The rate of change in the mass of water stored within the REV is:

$$\dot{M}_{st} = \dot{M}_w + \dot{M}_v \qquad \text{Equation 2}$$

where $\dot{M}_w$ and $\dot{M}_v$ represent the rate of change of liquid water and water vapor, respectively. The liquid water may contain dissolved solids and therefore have a density that is different from that of freshwater. The rate of change in the stored liquid water is given by:

$$\dot{M}_w = \frac{\partial(\rho_w \theta_w)}{\partial t} dx\, dy\, dz \qquad \text{Equation 3}$$

which can be expanded to:

$$\dot{M}_w = \rho_w \left(\theta_w \beta_w \frac{\partial u_w}{\partial t} + \beta \frac{\partial u_w}{\partial t} + m_w \frac{\partial \varphi}{\partial t} \right) + \theta_w \rho_w \alpha_w \frac{\partial T}{\partial t}$$ Equation 4

where ρ_w is the density of water, θ_w is the volumetric water content, β_w is the isothermal compressibility of water (~4.8E-10 m^2/N at 10 °C), u_w is the pore-water pressure, β is the soil structure compressibility, m_w is the slope of the volumetric water content function, and α_w is the volumetric coefficient of thermal expansion at constant pressure. The matric suction, φ, is the difference between pore-air pressure and pore-water pressure ($\varphi = u_a - u_w$).

The soil structure compressibility is equivalent to the inverse of the bulk modulus $(1/K)$ and links volumetric straining of the soil structure to changes in pore-water pressure. The specified soil compressibility must embody the loading conditions. For example, under three-dimensional loading conditions, the bulk modulus is related to the modulus of elasticity, E, and Poisson's ratio, ν, by the expression: $K = E/[3(1-2\nu)]$. Under two-dimensional plane strain loading conditions, the bulk modulus is expressed as $K = E/[(1+\nu)(1-2\nu)]$. Under one-dimensional loading conditions, the compressibility is equivalent to the coefficient of volume change, m_v, and the bulk modulus, which is often referred to as the constrained modulus for this loading condition, is related to the modulus of elasticity and Poisson's ratio by the expression: $K = E(1-\nu)/[(1+\nu)(1-2\nu)]$. Typical values of the elastic properties (E and ν) can be found in a number of textbooks on soil mechanics (e.g., Kézdi, 1974; Bowles, 1996).

The rate of change in the water vapor stored in the REV is calculated with the ideal gas law:

$$\dot{M}_v = \frac{\partial M_v}{\partial t} = \frac{M}{R} \frac{\partial}{\partial t} \left(\frac{p_v V_a}{T} \right) = \frac{M}{R} \frac{\partial}{\partial t} \left(\frac{p_v \theta_a}{T} \right) dx\, dy\, dz$$ Equation 5

where M is the molar mass, R is the gas constant (8.314472 J/K/mol), and p_v is the vapor pressure. The volume of air, V_a, is calculated using the volumetric air content ($\theta_a = n - \theta_w - \theta_{ice}$) multiplied by the volume of the REV ($dx\, dy\, dz$).

The total rate of change in the mass of water stored within the REV must be equal to the difference between the rate of mass inflow ($\dot{m}_{in}$) and the rate of mass outflow ($\dot{m}_{out}$). These rates of mass flow describe processes of water (liquid or vapor) transport across the REV control surfaces. All flows occur in response to energy gradients. In the case of liquid water, flow can occur due to mechanical (elastic potential, gravitational potential, kinetic), electrical, thermal, or chemical energy gradients; however, only mechanical energy gradients are considered by SEEP/W. Vapor flow can occur by diffusive transport due to partial vapor pressure gradients, or by advective transport with flowing air driven by gradients in total pressure and density in the bulk air phase (i.e., integrated with AIR/W).

The mass flow rate of liquid water in response to mechanical energy gradients can be described using Darcy's Law for a variable density fluid (e.g., Bear, 1979; Bear, 1988):

$$\dot{m}_w = \rho_w q_w dx dz = \frac{-K_w}{g} \left(\frac{\partial u_w}{\partial y} + \rho_w g \frac{\partial y}{\partial y} \right) dx dz$$ Equation 6

where q_w is the water flux, K_w is the isothermal liquid water hydraulic conductivity, and g is the acceleration due to gravity.

The mass flow rate of water vapor can be described using Fick's Law (e.g., Joshi et al., 1993; Nassar et al., 1989; Nassar et al., 1992; Saito et al., 2006):

$$\dot{m}_v = -D_v \frac{M}{R} \frac{\partial}{\partial t}\left(\frac{p_v}{T}\right) dxdz \qquad \text{Equation 7}$$

The coefficient of diffusion for water vapor in soil, D_v, is given by (Saito et al., 2006):

$$D_v = \tau \theta_a D_{vap} \qquad \text{Equation 8}$$

where τ is a tortuosity factor (e.g., Lai et al., 1976) and D_{vap} is the diffusivity of water vapor in air at a temperature specified in Kelvin (e.g., Kimball, 1976). Separation of the mass flow rate of water vapor into isothermal and thermal components yields (Philip and de Vries, 1957):

$$\dot{m}_v = -\left(\frac{K_{vU}}{g}\frac{\partial u_w}{\partial t} + \rho_w K_{vT}\frac{\partial T}{\partial t}\right) dxdz \qquad \text{Equation 9}$$

in which

$$K_{vU} = \frac{D_v}{\rho_w}\frac{p_{vo}^s M}{RT}\frac{Mg}{RT} h_s \qquad \text{Equation 10}$$

$$K_{vT} = \frac{D_v}{\rho_w}\frac{M}{RT} h_s \left(\frac{\partial p_{vo}^s}{\partial T} - \frac{p_{vo}^s u_w M}{\rho_w RT^2} - \frac{p_{vo}^s}{T}\right) \qquad \text{Equation 11}$$

where K_{vU} is the isothermal vapor conductivity, K_{vT} is the thermal vapor conductivity, and p_{vo}^s is the saturation vapor pressure. Substitution and expansion of the rate equations into the conservation statement and division by the dimensions of the control volume gives:

$$\rho_w\left(\theta_w\beta_w\frac{\partial u_w}{\partial t} + \beta\frac{\partial u_w}{\partial t} + m_w\frac{\partial}{\partial t}(u_a - u_w)\right) + \theta_w\rho_w\alpha_w\frac{\partial T}{\partial t} + \frac{\partial M_v}{\partial t} = \frac{\partial}{\partial y}\left[\left(\frac{K_w}{g} + \frac{K_{vU}}{g}\right)\frac{\partial u_w}{\partial t} + \rho_w K_w\frac{\partial y}{\partial y} + \rho_w K_{vT}\frac{\partial T}{\partial t}\right] \qquad \text{Equation 12}$$

Equation 12 can be simplified to the more conventional groundwater flow equation by ignoring vapor transfer and thermal expansion, and dividing by water density, which is assumed to be spatially and temporally constant:

$$(\theta_w\beta_w + \beta)\frac{\partial u_w}{\partial t} + m_w\frac{\partial(u_a - u_w)}{\partial t} = \frac{\partial}{\partial y}\left[\left(\frac{K_w}{\rho_w g}\right)\frac{\partial u_w}{\partial y} + K_w\frac{\partial y}{\partial y}\right] \qquad \text{Equation 13}$$

Equation 13 is further simplified for a saturated porous media by neglecting the second term (for changing saturation):

$$(\theta_w \beta_w + \beta)\frac{\partial u_w}{\partial t} = \frac{\partial}{\partial y}\left[\left(\frac{K_w}{\rho_w g}\right)\frac{\partial u_w}{\partial y} + K_w \frac{\partial y}{\partial y}\right] \qquad \text{Equation 14}$$

Table 3 provides a complete list of the physical processes included in the partial differential equation solved by SEEP/W.

Table 3. Summary of the physical processes included in the SEEP/W formulation.

Physical Process	GeoStudio Products
Storage: water compressibility	SEEP/W
Storage: soil structure compressibility	SEEP/W
Storage: change in saturation due to changes in matric suction arising from variation in pore-water pressure	SEEP/W
Storage: change in saturation due to changes in matric suction arising from variation in pore-air pressure	SEEP/W + AIR/W
Storage: thermal expansion/contraction	SEEP/W + TEMP/W
Storage: phase change by vaporization	SEEP/W
Flow: pressure-driven (isothermal)	SEEP/W
Flow: gravity-driven	SEEP/W
Flow: pressure-driven vapor flow (isothermal)	SEEP/W
Flow: thermally-driven vapor flow	SEEP/W + TEMP/W
Flow: density variations due to temperature distributions	SEEP/W + TEMP/W
Flow: density variations due to concentration distributions	SEEP/W + CTRAN/W

The key elements of the SEEP/W formulation are as follows:

- The default physical processes are pressure and gravity-driven flow, and storage changes due to water compressibility, soil structure compressibility, and changes in matric suction (i.e., drainage).
- Isothermal vapor transfer (vapor transfer in response to partial pressure gradients caused by spatial variations in pore-water pressure) is an optional physical process that does not require coupling with another GeoStudio product.
- Thermally driven vapor transfer (vapor transfer in response to partial pressure gradients caused by spatial variations in temperature) requires integration with TEMP/W.
- The vapor diffusion coefficient can represent either isothermal or non-isothermal conditions and is a derived material property calculated by the software (e.g., Saito et al. 2006).
- SEEP/W can be coupled with AIR/W to simultaneously model air transfer and its effect on water transfer and storage.

- In the absence of an air flow analysis, the pore-air pressure within an unsaturated soil is assumed to be at zero-gauge pressure. In this case, the matric suction is equal to the negative water pressure.
- Water flow in response to density gradients can be simulated by coupling SEEP/W with either TEMP/W (density changes in response to temperature) or CTRAN/W (density changes in response to concentration).
- The isothermal compressibility of water (β_w) is a property of the analysis, not a material model input.
- The volumetric coefficient of thermal expansion at constant pressure (α_w) is a property of the analysis, not a material model input. The coefficient is calculated by the software from a functional relationship between water density and temperature developed by the International Committee for Weights and Measures.
- The soil structure compressibility (β) is a material model input.
- Changes in storage due to soil structure compressibility are due solely to pore-water pressure changes; therefore, the total stresses within the domain are assumed constant.

3.2 Material Models

The material models in SEEP/W characterize the ability of a porous medium to store and transmit water. The transmission and storage properties for vapor are calculated automatically by the software, while the properties for liquid water are user inputs. The liquid water storage property defines the change in the stored mass of liquid water in response to pore-water pressure variation (Equation 4). The hydraulic conductivity function describes the ability of a soil to transmit water in response to the energy gradients (Equation 6).

3.2.1 Saturated-Only

Table 4 summarizes the inputs required by the saturated-only material model. Water storage changes are characterized by specifying the soil structure compressibility, which links volumetric straining of the soil structure to pore-water pressure variation (Equation 14). Under saturated conditions, the volumetric water content is equivalent to porosity. Section 3.2.4 elaborates on the definition of hydraulic anisotropy.

Table 4. Parameters for the saturated-only material model.

Parameter	Symbol	Unit
Hydraulic Conductivity	K_{sat}	m/s
Soil Structure Compressibility	β	m^2/kN or (1/kPa)
Saturated Volumetric Water Content	θ_w	
Anisotropy Ratio	$K_{y'}/K_{x'}$	
Anisotropy Ratio	$K_{z'}/K_{x'}$	
Dip Direction	γ	Degrees

Dip Angle	δ	Degrees

3.2.2 Saturated-Unsaturated

Table 5 summarizes the inputs for the saturated-unsaturated material model. The volumetric water content function characterizes the stored water volumes as a function of matric suction (φ), which, if air pressure is assumed to be zero, is equivalent to negative pore-water pressure. Hydraulic conductivity is a function of the volumetric water content, and therefore indirectly a function of pore-water pressure. Figure 1 presents an example of both functions. Section 3.2.4 elaborates on the definition of hydraulic anisotropy.

Table 5. Parameters for the saturated-unsaturated material model.

Parameter	Symbol	Unit
Hydraulic Conductivity Function	$K(u_w)$	m/s
Soil Structure Compressibility	β	m^2/kN or (1/kPa)
Volumetric Water Content Function	$\theta_w(u_w)$	
Anisotropy Ratio	$K_{y'}/K_{x'}$	
Anisotropy Ratio	$K_{z'}/K_{x'}$	
Dip Direction	γ	Degrees
Dip Angle	δ	Degrees

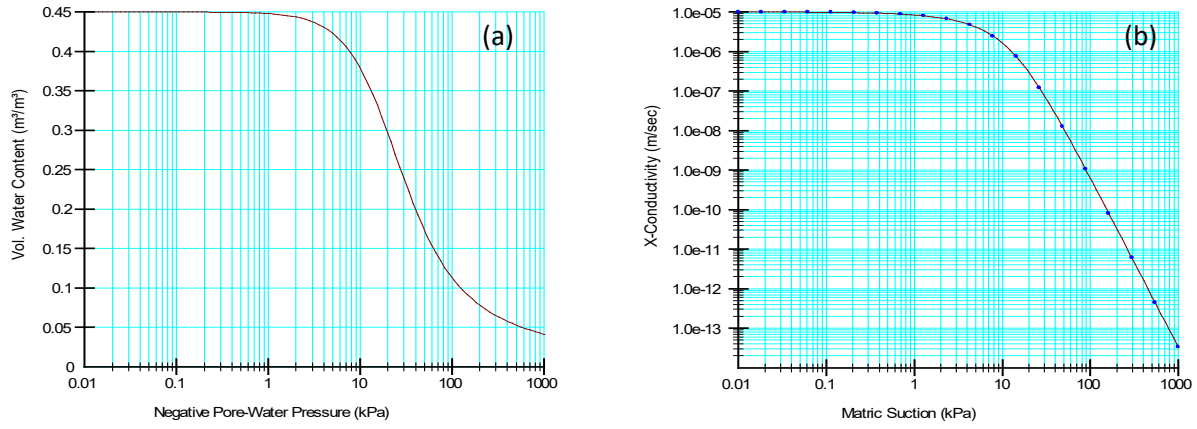

Figure 1. Examples of (a) volumetric water content and (b) hydraulic conductivity functions.

3.2.2.1 Hydraulic Conductivity of Frozen Ground

There is an option to reduce the hydraulic conductivity of the saturated-unsaturated material model when the soil freezes if a coupled water and heat transfer analysis is being completed. The change in

water pressure within the liquid water of a partially frozen soil can be determined from the Clapeyron thermodynamic equilibrium equation (Schofield, 1935; Williams and Smith, 1989):

$$\frac{\partial u_w}{\partial T} = \frac{h_{sf}}{v_w T_0} \qquad \text{Equation 15}$$

where ∂T is the change in temperature below the phase change temperature, h_{sf} is the latent heat of vaporization, v_w is the specific volume of water, and T_0 is the normal freezing point of water at atmospheric pressure. Equation 15 is used to calculate the reduction in pore-water pressure of the unfrozen liquid water, which is then used to determine the conductivity directly from the hydraulic conductivity function.

3.2.3 Estimation Techniques

3.2.3.1 Volumetric Water Content Function

GeoStudio provides several methods for estimating the volumetric water content function. Closed form equations requiring curve fit parameters can be used to generate the volumetric water content function according to techniques developed by Fredlund and Xing (1994):

$$\theta_w = C(\varphi)\frac{\theta_{sat}}{ln\left[e + \left(\frac{\varphi}{a}\right)^n\right]^m} \qquad \text{Equation 16}$$

or van Genuchten (1980):

$$\theta_w = \theta_{res} + \frac{\theta_{sat} - \theta_{res}}{[1 + (a'\varphi)^n]^m} \qquad \text{Equation 17}$$

where a, a', n, and m are curve fitting parameters that control the shape of the volumetric water content function, $C(\varphi)$ is a correlation function, θ_{sat} is the saturated volumetric water content, and θ_{res} is the residual volumetric water content. Note that the parameter a in Equation 16 has units of pressure and is related to the parameter a' ($a' = 1/a$), used by van Genuchten (1980) in Equation 17.

Sample volumetric water content functions are available for a variety of soil particle size distributions, ranging from clay to gravel. These sample functions are generated by using characteristic curve fit parameters in Equation 17. The volumetric water content function can also be estimated using the modified Kovacs model developed by Aubertin et al. (2003). The model requires grain size data including the diameter corresponding to 10% and 60% passing on the grain size curve (i.e., D_{10} and D_{60}), and the liquid limit. Finally, tabular data for volumetric water content and suction, obtained from the literature, estimated from other pedotransfer functions or from the results of laboratory testing, can be entered directly into the model.

3.2.3.2 Hydraulic Conductivity Function

GeoStudio provides two routines to estimate the hydraulic conductivity function from the saturated hydraulic conductivity and the volumetric water content function. The first is the Fredlund et al. (1994) equation:

$$K_w(\theta_w) = K_{sat} \int_{\theta_{res}}^{\theta_w} \frac{\theta_w - x}{\varphi^2(x)} dx \Big/ \int_{\theta_{res}}^{\theta_{sat}} \frac{\theta_{sat} - x}{\varphi^2(x)} dx \qquad \text{Equation 18}$$

where K_{sat} is the saturated hydraulic conductivity, x is a dummy variable of integration representing the water content, and the remainder of the symbols are defined in Section 3.2.3.1.

The second estimation method is the equation proposed by van Genuchten (1980). The parameters in the equation are generated using the curve fitting parameters from the volumetric water content function and an input value for saturated hydraulic conductivity. The closed-form equation for hydraulic conductivity is as follows:

$$K_w(\varphi) = K_{sat} \frac{\{1 - (a'\varphi)^{n-1}[1 + (a'\varphi)^n]^{-m}\}^2}{[1 + (a'\varphi)^n]^{\frac{m}{2}}} \qquad \text{Equation 19}$$

3.2.4 Anisotropy

The hydraulic conductivity of porous media is often higher in one direction than in other directions. This directional dependency (i.e., anisotropy) is generally due to sedimentation, consolidation, dissolution, and/or homogenization of layered media as equivalent homogeneous media. In these cases, the hydraulic conductivity is assumed orthotropic; that is, unique, and independent, in three mutually perpendicular directions. The hydraulic conductivity is known along the principal axes (X', Y', Z') of the rotated Cartesian coordinate system (Figure 2).

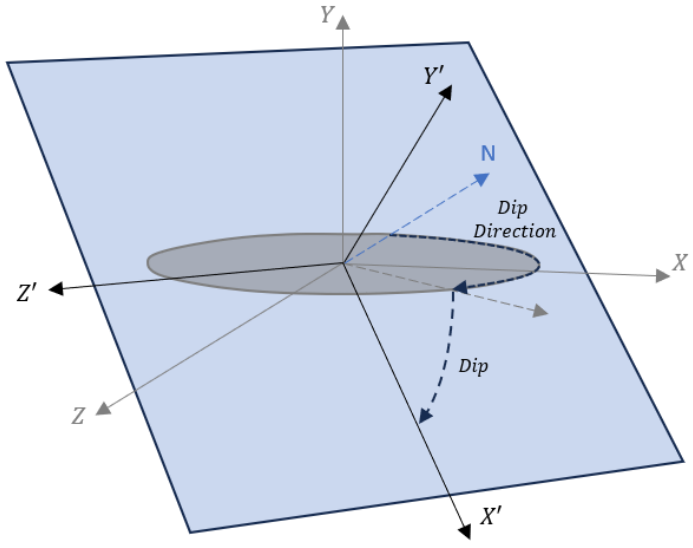

Figure 2. Rotation of the principal conductivity axes.

The user-entered value for the conductivity represents the value along the X'-axis (i.e., $K_{x'}$). The anisotropy ratios $K_{y'}/K_{x'}$ and $K_{z'}/K_{x'}$ are used to calculate $K_{y'}$ and $K_{z'}$ from $K_{x'}$. The dip angle (δ) and direction (γ) are used to locate the principal axes of the rotated Cartesian coordinate system (Figure 2). Dip angle and dip direction is a measurement convention used to describe the orientation of a planar feature. The dip angle is the steepest angle of descent of a tilted feature relative to a horizontal plane. The dip direction is the azimuth (i.e., compass direction) of the dip line of the planar feature; that is, the azimuth of the imagined line inclined downslope. Dip is always entered as a positive value between $0°$ and $90°$. Dip direction, being an azimuth, is clockwise positive from North. In GeoStudio, North is aligned with the negative Z-axis.

In a two-dimensional analysis (Figure 3), the domain is in the $X - Y$ plane, North is in the out-of-plane direction (i.e., into the page), and an input dip direction of $0° \leq \gamma \leq 180°$ is set to $\gamma = 90°$ by the solver (i.e., $+X$ direction; East) while $180° < \gamma < 360°$ is set $\gamma = 270°$ by the solver (i.e., $-X$ direction; West). The anisotropy ratio $K_{z'}/K_{x'}$ therefore has no effect on the solution.

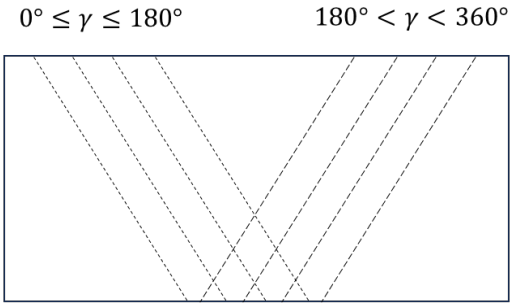

Figure 3. Interpretation of dip direction (γ) in a 2D analysis.

If the two-dimensional section is at an oblique angle (β') relative to the dip direction (Figure 4), the dip angle can be replaced by an apparent dip angle $\alpha = \tan^{-1}(\cos\beta' \tan\delta)$.

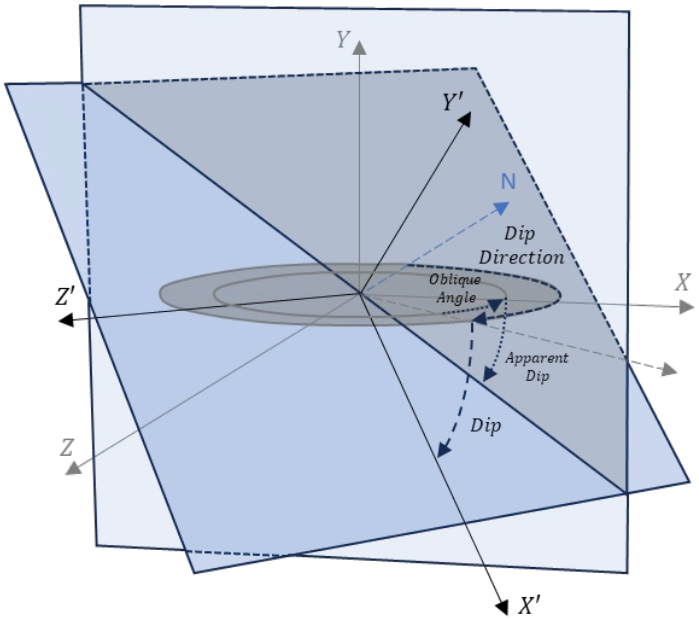

Figure 4. Interpretation of dip and apparent dip.

3.3 Boundary Conditions

The solution of the FEM equations is constrained by boundary conditions specified across the domain. These boundary conditions generally take the form of the dependent variables (1st type boundary condition) or the gradient of the dependent variable (2nd type boundary condition) normal to the boundary. The 2nd type boundary condition is generally expressed in terms of the water flow rate across the boundary. The case of a zero-flow boundary is a special case in which the gradient of the dependent variable normal to the boundary is set to zero. The zero-flow boundary is the default boundary condition, since all nodes have zero net flow in the absence of a source or sink, according to the conservation of mass statement. Thus, the zero-flow boundary condition is assumed when there is no boundary condition specified at an exterior node.

The basic 1st and 2nd type boundary conditions are generally self explanatory and the means of defining them are described in the example files and tutorials. However, the more complex boundary conditions merit further discussion and are described in the following sections.

3.3.1 Potential Seepage Face Review

The potential seepage face review boundary should be used if a free surface (i.e., pressure equal to zero) may develop along the boundary. For example, this condition can be used to simulate water discharging along a portion of the downstream side of an earth structure or flow into an unpressurized drain. A seepage face review is also required if the applied water flux boundary condition is in excess of the infiltration capacity of the soil. The review process ensures that the maximum pore-water pressure along the discharge surface or on the infiltration boundary is zero. A potential seepage face review can be completed when using the following boundary conditions: total head, water flux, water rate, and total head versus volume.

3.3.2 Total Head versus Volume

The water level within a topographic low or basin can vary over time as water flow across the ground surface causes the height of ponded water to change. The water level in a pond or lake, for example, might increase if there is groundwater discharge (Figure 5). A similar situation develops during a falling head test within a standpipe well. The rate at which the water level in the well drops depends on the rate of flow across the screen.

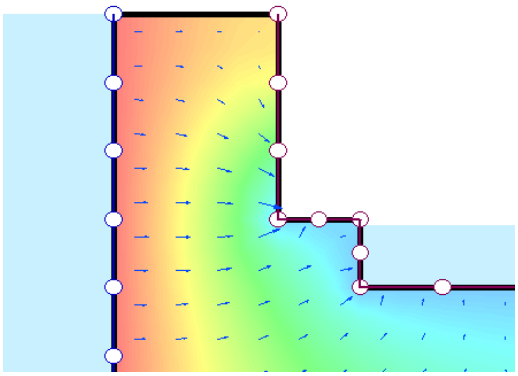

Figure 5. Example of the Total Head versus Volume boundary condition applied to the inside of an excavation.

These types of scenarios can be modelled using a total head versus cumulative volume boundary condition. When this boundary condition is applied, SEEP/W will automatically adjust the total head within an irregularly shaped depression as water flows into or out of the domain, based on the cumulative volume of flow across the boundary and the geometry of the topographic surface. Alternatively, the relationship between total head and cumulative flow volumes (into or out of the domain) can be defined *a priori* for well-defined geometries (e.g., a constructed pond or the riser pipe of a well).

3.3.3 Unit Gradient

Water that enters the ground surface and passes beyond an upper active zone to enter the deeper groundwater system is considered recharge or deep/net percolation. In uniform, deep, unsaturated zones, the gravity gradient becomes the dominant gradient responsible for net percolation. In this situation, the hydraulic gradient is equal to the elevation gradient (dy/dy), which is always 1.0. Since the vertical hydraulic gradient produced by gravity is unity, the rate of net percolation and the hydraulic conductivity become numerically equal and the pore-water pressures remain relatively constant with depth. Under these conditions, Darcy's Law can be written as follows (after Equation 6):

$$q_w = -K_w\left(\frac{\partial u_w}{\partial y} + \frac{\partial y}{\partial y}\right) = -K_w(0.0 + 1.0) = -K_w \qquad \text{Equation 20}$$

The unit gradient boundary condition can be applied to the lower boundary of a domain when the negative pore-water pressure (suction) is assumed to be constant with depth. However, this assumption does not require that suction is constant with time because a change in the flux associated with net percolation will affect suction even under the unit gradient conditions.

3.3.4 Land-Climate Interaction

SEEP/W can simulate Soil-Vegetation-Atmosphere-Transfers across the ground surface using the land-climate interaction (LCI) boundary condition. The LCI boundary condition can reflect various ground surface conditions including bare, snow-covered, or vegetated ground. A boundary condition of this type can be used to compute the water balance and net percolation through an engineered cover system or evaluate the ability of a cover system to provide sufficient water for long-term plant growth.

3.3.4.1 Surface Mass Balance Equation

The water flux at the ground surface can be calculated with a mass balance equation:

$$(q_P + q_M)cos\alpha + q_E + q_R = q_I \qquad \text{Equation 21}$$

where superscripts on the water fluxes (q) indicate rainfall (P), snow melt (M), infiltration (I), evaporation (E) and runoff (R), and α is the slope angle. Rainfall is only considering during solve-time if the air temperature is above freezing. The slope angle is used to convert a vertical flux (i.e., P and M) to a flux normal to the boundary. The evaporation and runoff fluxes are negative; that is, out of the domain. Infiltration is the residual of the mass balance equation and forms the boundary condition of the water transfer equation. Transpiration does not appear in Equation 18 because root water uptake occurs below the ground surface.

If the applied infiltration flux results in ponding, the pore-water pressure is set to zero and the time step is resolved. Runoff is then calculated at the end of the time step as:

$$q_R = q_I^{sim} - (q_P + q_M)cos\alpha - q_E \quad \text{Equation 22}$$

where q_I^{sim} is the simulated infiltration flux.

The maximum amount of evapotranspiration at a site is defined by the potential evapotranspiration (PET). This potential rate of water transfer is partitioned into potential evaporation (PE) and potential transpiration (PT) based on the soil cover fraction (SCF). SCF varies from 0.0 for bare ground to 1.0 for a heavily vegetated surface. The proportion of PET attributed to potential surface evaporation is:

$$q_{PE} = q_{PET}(1 - SCF) \quad \text{Equation 23}$$

while the portion that is potential transpiration flux is:

$$q_{PT} = q_{PET}(SCF) \quad \text{Equation 24}$$

Equation 24 is used to calculate root water uptake. The evaporation flux at the ground surface rarely equals the potential evaporation due to limited water availability. The evaporation flux in Equation 21 is calculated by recasting Equation 23 as:

$$q_E = q_{AE}(1 - SCF) \quad \text{Equation 25}$$

where q_{AE} is the actual evaporation. The user has the option to allow evaporation to occur during rainfall events.

Ritchie (1972) proposed the following equation, based on the interception of solar radiation by the vegetation canopy, to apportion PET into PE and PT:

$$SCF = 1 - e^{-k(LAI)} \quad \text{Equation 26}$$

where LAI is the leaf area index and k is a constant governing the radiation extinction by the canopy as a function of the sun angle, distribution of plants, and arrangement of leaves. The value of k is generally between 0.5 and 0.75. Various expressions exist for estimating LAI from crop height.

3.3.4.1.1 Calculation of Evapotranspiration

Modelling evaporative flux at the ground surface (Equation 22 and Equation 25) requires knowledge of the actual evaporation, while modelling root water uptake via Equation 24 requires the potential evapotranspiration. There are three 'Evapotranspiration' methods available in SEEP/W: 1) user-defined; 2) Penman-Wilson; and, 3) Penman-Monteith.

The potential evapotranspiration is *specified* as a function of time for method 1. The actual evaporation is calculated using the relationship proposed by Wilson et al. (1997):

$$q_{AE} = q_{PET}\left[\frac{p_v^s - p_v^a}{p_{v0}^s - p_v^a}\right] \qquad \text{Equation 27}$$

where p_v^s and p_v^a are the vapor pressures at the surface of the soil and the air above the soil, respectively, and p_{v0}^s is the vapor pressure at the surface of the soil for the saturated condition (kPa). The term in brackets, which is referred to as the limiting function (LF), is a ratio of the actual vapor pressure deficit to the potential vapor pressure deficit for a fully saturated soil. The user input, q_{PET}, can be determined from measured data or empirical and semi-empirical methods such as Thornthwaite (1948) and Penman (1948).

The second method, the Penman-Wilson method, is based on the modification of the well-known Penman (1948) equation used to calculate potential evaporation. The Penman-Wilson method calculates the *actual* evaporation from the bare ground surface as (Wilson et al., 1997):

$$q_{AE} = \frac{\Gamma q_n^* + \gamma E_a}{\Gamma + \gamma/h_s} \qquad \text{Equation 28}$$

where the aridity, E_a, is given as:

$$E_a = [2.625(1 + 0.146u)]p_v^a\left({}^1/_{h_a} - {}^1/_{h_s}\right) \qquad \text{Equation 29}$$

and

h_a	Relative humidity of the air
h_s	Relative humidity of the soil
Γ	Slope of the saturation vapor pressure verses temperature curve
q_n^*	Net radiation in terms of water flux
γ	Psychrometric constant = 0.0665 kPa/C
u	Wind speed

The Penman-Wilson equation calculates potential evapotranspiration by substituting a relative humidity of 1.0 into Equation 28, which causes the equation to revert to the original Penman equation (Penman, 1948). Calculation of the relative humidity at the ground surface (h_s) requires temperature and matric suction. A heat transfer analysis (TEMP/W) can be used to compute the temperature at the ground surface; otherwise, the ground temperature is assumed to be equal to the air temperature.

Monteith extended the original work of Penman to crop surfaces by introducing resistance factors. The Penman-Monteith equation (method 3) for calculating potential evapotranspiration, q_{PET}, is well accepted in the soil science and agronomy fields and is the recommended procedure of the Food and Agriculture Organization of the United Nations (Allen et al., 1998). This method is generally best for vegetated systems where transpiration dominates over evaporation.

The Penman-Monteith equation separates potential evapotranspiration into radiation and aerodynamic terms, and is considered a combined model (energy balance and aerodynamic method):

$$q_{PET} = q_{PET}^{rad} + q_{PET}^{aero} = \frac{1}{h_{fg}}\left[\frac{\Gamma(q_n - q_g)}{\Gamma + \gamma\left(1 + \frac{r_c}{r_a}\right)} + \frac{\rho_a c_{sa} \left(p_{v0}^a - p_v^a\right)/r_a}{\Gamma + \gamma\left(1 + \frac{r_c}{r_a}\right)}\right] \quad \text{Equation 30}$$

where

q_{PET}	Potential evaporation flux
h_{fg}	Latent heat of vaporization
q_n	Net radiation
q_g	Ground heat flux
ρ_a	Mean air (atmospheric) density
c_{sa}	Specific heat of moist air
$(p_{v0}^a - p_v^a)$	Vapor pressure deficit
p_{v0}^a	Saturated vapor pressure at the mean air temperature
p_v^a	Actual vapor pressure of the air at a reference height
r_c	Bulk surface (crop canopy) resistance
r_a	Aerodynamic resistance

The radiation term considers the difference between the net radiation flux and the ground heat flux, while the aerodynamic term considers the vapor pressure deficit. The aerodynamic resistance controls the transfer of water vapor from the evaporating surface into the air above the canopy and is given by (Allen et al., 1998):

$$r_a = \frac{1}{uk^2}\left[ln\left(\frac{z_{ref} - d}{z_{om}}\right)\right]\left[ln\left(\frac{z_{ref} - d}{z_{oh}}\right)\right] \quad \text{Equation 31}$$

where

u	Wind speed
k	von Karman's constant = 0.41
z_{ref}	height of wind, humidity, temperature measurements (generally at 1.5 m)
$d = (2/3)z_c$	Zero-plane displacement height of the wind profile
$z_m = (0.123)z_c$	Surface roughness height for momentum flux
$z_h = 0.1z_m$	Surface roughness height for heat and vapor flux
z_c	Crop height

The zero-plane displacement height and surface roughness parameter for momentum are generally assumed to be some fraction of the vegetation height. The roughness parameter for heat and water vapor is assumed to be a fraction of the roughness parameter for momentum (Allen et al., 1998; Dingman, 2008; Saito and Simunek, 2009).

The crop canopy resistance controls water vapor transfer through the transpiring crop and can be estimated by (Allen et al., 1998):

$$r_c = \frac{r_l}{0.5LAI} = \frac{100}{0.5LAI} = \frac{200}{LAI} \qquad \text{Equation 32}$$

where r_l is bulk stomatal resistance of the well-illuminated leaf. The LAI cannot be zero (bare ground) in Equation 32, so a minimum of 0.1 is imposed in SEEP/W.

Potential evapotranspiration is calculated for a vegetated surface of any height. The potential evapotranspiration value is then apportioned into evaporative and transpiration fluxes, using Equation 23 and Equation 24. As such, method 3 does not reduce PE to AE based on water availability. It is worth noting that the crop canopy resistance approaches infinity as the LAI approaches zero. Thus, the Penman-Monteith equation does not adequately represent evaporation-dominant systems.

3.3.4.1.2 Root Water Uptake

SEEP/W determines the root water uptake as part of the LCI boundary condition if vegetation characteristics have been defined. A general equation for the maximum possible root water extraction rate per volume of soil, q_{root}^{max}, over a root zone of arbitrary shape is given by (Feddes et al., 2001):

$$q_{root} = \pi'_{root} \alpha_{rw} q_{PT} \qquad \text{Equation 33}$$

where α_{rw} is a reduction factor due to water stress, q_{PT} is equal to the potential transpiration flux, and π'_{root} is the normalized water uptake distribution. The potential transpiration flux is computed using Equation 24. The reduction factor is defined by a plant limiting function, which is a functional relationship between the reduction factor and matric suction. Equation 33 is uniquely calculated at each gauss point within the root zone.

The normalized water uptake distribution is:

$$\pi'_{root} = \frac{\pi_{root}}{\int_0^{r_{max}} \pi_{root}\, dr} \qquad \text{Equation 34}$$

where π_{root} is the root length density or the length of root per volume of soil. Integration of the root density function over the maximum root depth, r_{max}, gives the total root length beneath a unit area. Normalizing the uptake distribution ensures that the normalized water uptake distribution is unity over the maximum root depth:

$$\int_0^{r_{max}} \pi'_{root}\, dr = 1.0 \qquad \text{Equation 35}$$

Finally, integration of Equation 33 over the rooting depth recovers the actual transpiration flux:

$$q_{AT} = \int_0^{r_{max}} q_{root}\, dr \qquad \text{Equation 36}$$

3.3.4.1.3 Snow Melt

The LCI boundary condition in SEEP/W calculates the water flux associated with snowmelt (in Equation 21) based on the change in snow pack depth between time steps:

$$q_M = \frac{\Delta h_{snow}}{\Delta t}\frac{\rho_{snow}}{\rho_w} \qquad \text{Equation 37}$$

where Δh_{snow} is the change in snow depth, Δt is the time increment, and ρ_{snow} is the snow density. A snow depth verses time function is required to calculate snowmelt flux. Snow depth data can be measured or estimated using a temperature-index method (see examples).

3.3.4.1.4 Minimum Pore-Water Pressure

The LCI boundary condition in SEEP/W prevents over-drying via a Calculated or User-Defined minimum pore-water pressure function. The relative humidity h_r at the soil-air interface is given by the thermodynamic relationship:

$$h_r = exp[u_w M/(\rho_w RT)] \qquad \text{Equation 38}$$

where M is the molecular mass of water, ρ_w fresh water density, R universal gas constant, and T absolute temperature. Solving for the minimum (negative) pore-water pressure u_w^{min} that could develop for a known air relative humidity gives:

$$u_w^{min} = \frac{\rho_w RT}{M} ln(h_r) \qquad \text{Equation 39}$$

3.3.4.2 Inputs

Table 6 presents the LCI inputs for the three different evapotranspiration methods. All three methods require functions for air temperature, precipitation, and relative humidity over time. Snow depth and snow density are optional, although the later must be defined if snowmelt is to be modelled. The Penman-Wilson and Penman-Monteith equations require wind speed and net radiation. SEEP/W provides an option to select solar radiation (incoming) so that net radiation is calculated during solve-time (see Section 4.3.1). The Penman-Monteith equation requires vegetation height. Finally, the user-defined option requires that potential evapotranspiration is specified over time.

Table 6. Inputs for the land-climate interaction boundary condition.

Evapotranspiration Method	Inputs
All	Air temperature versus time Precipitation flux versus time Relative humidity Snow depth versus time (optional) Snow density (optional)
Penman-Wilson & Penman-Monteith	Wind speed versus time Net radiation versus time
Penman-Monteith	Vegetation height versus time
User-Defined	Potential evapotranspiration versus time

Table 7 presents the vegetation data inputs required for modelling root water uptake. All evapotranspiration methods require inputs for leaf area index, plant moisture limiting, root depth, normalized root density, and soil cover fraction.

Table 7. Inputs for root water uptake.

Evapotranspiration Method	Inputs
All	Leaf area index versus time Plant moisture limiting function Root depth versus time function Normalized root density Soil cover fraction versus time function

3.3.5 Diurnal Distributions

3.3.5.1 Air Temperature

The air temperature at any hour of the day can be estimated from the daily maximum and minimum values with:

$$T_a = \frac{T_{max} + T_{min}}{2} + \frac{T_{max} - T_{min}}{2} cos\left[2\pi\left(\frac{t-13}{24}\right)\right] \quad \text{Equation 40}$$

where T_{max} and T_{min} are the daily maximum and minimum temperatures, respectively, and t is the time in hours since 00:00:00. The approximation, which is used by Šimůnek et al. (2012) and presented by Fredlund et al. (2012), assumes the lowest and highest temperature to occur at 01:00 and 13:00, respectively. Equation 40 provides a continuous variation of the air temperature throughout the day; however, the diurnal distributions are discontinuous from day-to-day. A continuous function over multiple days is obtained by calculating T_a for $t > 13{:}00$ using T_{min} from the subsequent day.

3.3.5.2 Relative Humidity

The relative humidity at any hour of the day can be estimated from the measured daily maximum and minimum values in the air:

$$h_a = \frac{h_{max} + h_{min}}{2} + \frac{h_{max} - h_{min}}{2} cos\left[2\pi\left(\frac{t-1}{24}\right)\right] \quad \text{Equation 41}$$

where h_{max} and h_{min} are the daily maximum and minimum relative humidity, respectively, and t is the time in hours since 00:00:00. The approximation, which is used by Šimůnek et al. (2012) and presented by Fredlund et al. (2012), assumes the lowest and highest relative humidity to occur at 13:00 and 01:00, respectively, which are the opposite times as the air temperature peaks. Equation 41 provides continuous variation of the relative humidity throughout the day; however, the diurnal distributions are discontinuous from day-to-day. Similar to the temperature function, the relative humidity function is continuous over multiple days if h_a for $t > 13{:}00$ is calculated with h_{max} from the subsequent day.

3.3.5.3 Daily Potential Evapotranspiration

User-defined daily PET values can be distributed across the day in accordance with diurnal variations in net radiation. Fayer (2000) assumes the fluxes are constant between about 0 to 6 hours and 18 to 24 hours, and otherwise follow a sinusoidal distribution:

$$q_{PET} = 0.24(\overline{q_{PET}}) \qquad t < 0.264\ d; t > 0.736\ d \qquad \text{Equation 42}$$

and

$$q_{PET} = 2.75(\overline{q_{PET}})sin\left(2\pi t - \frac{\pi}{2}\right) \qquad 0.264\ d \le t \le 0.736\ d \qquad \text{Equation 43}$$

where the daily average potential evapotranspiration flux, $\overline{q_{PET}}$, is expressed with the same time units as the time variable. Equation 42 and Equation 43 produce a continuous function of instantaneous flux. A finite element formulation is discretized in time and assumes the flux constant over the time step. GeoStudio therefore obtains the potential evaporation flux by numerically integrating the function between the beginning and end of the step and dividing by the time increment.

3.3.6 Estimation Techniques

3.3.6.1 Snow Depth

Snow depth on the ground surface at any instant in time, h_{snow}, is the summation of all incremental snow depth accumulations minus snowmelt:

$$h_{snow} = \sum_{0}^{t} (\Delta h_{snow} - \Delta h_{melt}) \qquad \text{Equation 44}$$

where Δh_{snow} is the incremental snow depth accumulation corrected for ablation and Δh_{melt} represents the snowmelt over a given period.

Snow accumulation models often use temperature near the ground surface to determine the fraction of precipitation falling as rain or snow (e.g., SNOW-17, Anderson, 2006). SEEP/W sets the fraction of precipitation occurring as snow, f_s, to 1.0 if the average air temperature over the time interval is less than or equal to the specified threshold temperature. Conversely, the snow fraction is set to 0.0 if the average air temperature over the time interval was greater than the threshold value. The threshold temperature is a model input.

Snow accumulation over the time interval in terms of snow-water equivalent, Δh_{swe}, is determined by:

$$\Delta h_{swe} = h_P \times f_s \times MF \qquad \text{Equation 45}$$

where h_P is the precipitation depth (liquid) over the time interval, and MF is a multiplier factor determined from the ablation constant as:

$$MF = 1 - Ablation\ Constant \qquad \text{Equation 46}$$

The snow depth accumulated over the interval is then calculated as:

$$\Delta h_{snow} = \Delta h_{swe} \frac{\rho_w}{\rho_{snow}}$$ Equation 47

where the snow density, ρ_{snow}, is input as a model parameter.

Snowmelt is assumed to only occur when the average air temperature is greater than 0°C. The daily snow melt depth, a model input, is used to compute snowmelt rate for a given time interval.

3.4 Convergence

3.4.1 Water Balance Error

The transient water transfer equation is formulated from the principle of mass conservation. As such, an apparent water balance error can be calculated by comparing the cumulative change in stored mass to the cumulative mass of water that flowed past the domain boundaries. The error is 'apparent' because it is a mathematical by-product of non-convergence, not an actual loss of mass, since the solution conserves mass.

The software allows for inspection of mass balance errors on sub-domains. Sub-domains are essentially control volumes that comprise a group of elements. The elements undergo changes in stored mass during a transient analysis. Water enters or exits the sub-domain at nodes on the boundary of the sub-domain and nodes inside the domain to which boundary conditions are applied (e.g., root water uptake).

The cumulative mass of water that enters the domain, $\dot{m}_{in}$, minus the mass of water that leaves the domain, $\dot{m}_{out}$, plus the mass of water that is added to (or removed from) the domain, $\dot{M}_S$, can be calculated by reassembling the forcing vector:

$$\int_0^t \left(\dot{m}_{in} - \dot{m}_{out} + \dot{M}_S\right) dt = \sum_0^t \dot{R} dt$$ Equation 48

The rate of increase in the mass of water stored within the domain is:

$$\int_0^t \dot{M}_{st}\, dt$$ Equation 49

The change in stored mass (Equation 49) is calculated in accordance with the final solution and all of the storage terms shown in Equation 12 and/or listed in Table 3 (e.g., thermal expansion of water). The calculated mass balance error is the difference between Equation 49 and Equation 48. The relative error is calculated by dividing the absolute error by the maximum of Equation 48 or Equation 49.

3.4.2 Conductivity Comparison

Convergence can also be assessed by comparing the input hydraulic conductivity functions to a scatter plot of the hydraulic conductivities from the penultimate iteration and the final pore water pressures. The points of the scatter plot will generally overlie the input hydraulic functions if the solution did not change significantly on the last two iterations. However, discrepancies might remain if the input functions are highly non-linear, even if the changes in pore-water pressures were negligible and the convergence criteria were satisfied (Section I.8). Therefore, evaluating convergence of non-linear hydraulic properties requires multiple pieces of information. In addition, a less-than-perfect match between the scatter plot and the input functions may sometimes be acceptable in the context of the modelling objectives or in light of other convergence criteria.

4 Heat Transfer

TEMP/W (or TEMP3D) is a finite element program for simulating heat transfer through porous media. Typical applications of TEMP/W include studies of naturally occurring frozen ground (e.g., permafrost), artificial ground freezing (e.g., for ground stabilization or seepage control), and frost propagation (e.g., for insulation design for structures or roadways). Section 4.1 summarizes the heat transfer and storage processes that are included in the formulation, while Section 4.2 describes the constitutive models available to characterize the properties of the medium and Section 4.3 describes the boundary conditions unique to TEMP/W.

4.1 Theory

The TEMP/W formulation is based on the law of energy conservation or the first law of thermodynamics, which states that the total energy of a system is conserved unless energy crosses its boundaries (Incropera et al., 2007). Similarly, the rate of change of stored thermal energy within a specified volume must be equal to the difference in the rate of heat flux into and out of the volume, as described in the following equation:

$$\dot{E}_{st} \equiv \frac{dE_{st}}{dt} = \dot{E}_{in} - \dot{E}_{out} + \dot{E}_g \qquad \text{Equation 50}$$

where $\dot{E}_{st}$ is the rate of change in the stored thermal energy, the inflow and outflow terms, $\dot{E}_{in}$ and $\dot{E}_{out}$, represent the rate of change in heat flux across the control surfaces, and $\dot{E}_g$ is a heat sink or source within the control volume ($dx\ dy\ dz$).

In a porous medium containing water, the rate of change in the thermal energy stored in this volume is:

$$\dot{E}_{st} = \dot{U}_{sens} + \dot{U}_{lat} = \dot{U}_{sen} + \dot{U}_{sf} + \dot{U}_{fg} \qquad \text{Equation 51}$$

where $\dot{U}_{sens}$ and $\dot{U}_{lat}$ represent the rate of change in the thermal energy associated with sensible and latent heat, respectively, in the control volume. The rate of change in the sensible energy is equal to (e.g., Andersland and Ladanyi, 2004):

$$\dot{U}_{sens} = C_p \frac{\partial T}{\partial t} dx\ dy\ dz \qquad \text{Equation 52}$$

where C_p is the volumetric heat capacity associated with the control volume. Volumetric heat capacity is the summation of the product of specific heat capacity, c_p, mass density, ρ, and volumetric fraction, θ, of each component in the control volume (i.e., solid particles, water, ice, and air).

The change in latent energy within the control volume could be due to fusion, $\dot{U}_{sf}$ (conversion from solid to liquid or liquid to solid, via freezing or melting), or due to vaporization, $\dot{U}_{fg}$ (conversion from liquid to gas or vice versa, via evaporation or condensation). The latent heat of fusion, h_{sf}, and vaporization, h_{fg}, represent the amount of energy required per unit mass of substance (i.e., water) to effect these changes in state.

The rate of change in the latent energy associated with fusion for water is:

$$\dot{U}_{sf} = -h_{sf}\frac{\partial M_{ice}}{\partial t} = -\rho_{ice}h_{sf}\frac{\partial \theta_{ice}}{\partial t}dx\,dy\,dz \qquad \text{Equation 53}$$

where M_{ice} is the mass of ice in the control volume, θ_{ice} is the volumetric ice content, and ρ_{ice} is the mass density of ice.

The rate of change in the latent energy associated with vaporization is given by:

$$\dot{U}_{fg} = h_{fg}\frac{\partial M_v}{\partial t} \qquad \text{Equation 54}$$

where M_v is the mass of vapor in the control volume. An increase in the mass of vapor is associated with an increase in latent energy within the control volume. Energy is released into the control volume during condensation and is consumed from within the control volume during vaporization.

The inflow and outflow terms ($\dot{E}_{in}$ and $\dot{E}_{out}$) are associated exclusively with processes occurring at the control surfaces. TEMP/W considers heat transfer across the boundaries via heat conduction and advection. The rate of change in energy associated with conduction is described by Fourier's Law (e.g., Carslaw and Jaeger, 1986):

$$\dot{Q}_y = -k\frac{\partial T}{\partial y}dxdz \qquad \text{Equation 55}$$

where k is the thermal conductivity of the medium.

Advection occurs when water entering or leaving the control volume transports thermal energy. The advective heat flux may be comprised of both sensible and latent energy transfers. The net rate at which sensible thermal energy enters the control volume with the flow of liquid water, water vapor, and (dry) air can be calculated from the respective mass flow rates, $\dot{m}$:

$$\left(\frac{\partial\left(\dot{m}_y u_{t(y)}\right)}{\partial y}\right)_{sens} = c_w\frac{\partial(\dot{m}_w T)}{\partial y} + c_v\frac{\partial(\dot{m}_v T)}{\partial y} + c_a\frac{\partial(\dot{m}_a T)}{\partial y} \qquad \text{Equation 56}$$

where $u_{t(y)}$ is the sensible thermal energy per unit mass calculated as the product of the temperature and specific heat, c, with subscripts indicating water, vapor, and air.

Transport of vapor from one location to another constitutes a transport of energy in latent form because evaporation or condensation within soil liberates or consumes heat energy (Jury and Horton, 2004). The rate of change in the latent energy due to vapor transfer into the control volume can be computed by:

$$\left(\frac{\partial\left(\dot{m}_y u_{t(y)}\right)}{\partial y}\right)_{lat} = h_{fg}\frac{\partial \dot{m}_v}{\partial y} \qquad \text{Equation 57}$$

where $\dot{m}_v$ represents the mass flow rate of water vapor entering the control volume.

Substitution and expansion of the foregoing rate equations into the conservation statement and division by the dimensions of the control volume gives the convective form of the heat transfer equation:

$$\left(C_p + \rho_w h_{sf} \frac{\partial \theta_{uwc}}{\partial T}\right)\frac{\partial T}{\partial t} + h_{fg}\frac{\partial M_v}{\partial t} = \frac{\partial}{\partial y}\left(k\frac{\partial T}{\partial y}\right) - c_w\frac{\partial\left(\dot{m}_w^{"}T\right)}{\partial y} - c_v\frac{\partial\left(\dot{m}_v^{"}T\right)}{\partial y} - c_a\frac{\partial\left(\dot{m}_a^{"}T\right)}{\partial y} - h_{fg}\frac{\partial \dot{m}_v^{"}}{\partial y}$$ Equation 58

where the double prime indicates a mass flux and θ_{uwc} is the unfrozen volumetric water content. Equation 58 can be simplified by ignoring forced-convection heat transfer and the latent heat of vaporization, giving:

$$C_{ap}\frac{\partial T}{\partial t} = \frac{\partial}{\partial y}\left(k\frac{\partial T}{\partial y}\right)$$ Equation 59

where the apparent volumetric heat capacity, C_{ap} , is defined as:

$$C_{ap} = C_p + \rho_w h_{sf}\frac{\partial \theta_{uwc}}{\partial T}$$ Equation 60

Table 8 provides a complete list of the physical processes included in the partial differential equation solved by TEMP/W.

Table 8. Summary of the physical processes included in the TEMP/W formulation.

Physical Process	GeoStudio Products
Storage: sensible energy	TEMP/W
Storage: latent heat of fusion (freeze/thaw)	TEMP/W
Storage: latent heat of vaporization (vaporization/condensation)	TEMP/W + SEEP/W
Flow: conduction	TEMP/W
Flow: sensible heat advection with water transfer	TEMP/W + SEEP/W
Flow: sensible heat advection with vapor transfer	TEMP/W + SEEP/W
Flow: sensible heat advection with air transfer	TEMP/W + SEEP/W + AIR/W
Flow: net latent energy transfer	TEMP/W + SEEP/W

The key elements of the TEMP/W formulation are as follows:

- The default physical processes in TEMP/W include conduction heat transfer and changes in stored sensible energy and latent heat of fusion.

- Advection heat transfer with flowing water and air – also referred to as forced convection – can be simulated by coupling TEMP/W with SEEP/W and AIR/W, respectively.
- A SEEP/W analysis that includes vapor transfer is required to evaluate the effects of vapor on heat transfer.
- The latent heat of vaporization, h_{sf}, and temperature at which phase change occurs are properties of the analysis, not a material model input.

4.2 Material Models

The TEMP/W material models characterize the ability of a porous medium to store and transmit heat. The soil storage property quantifies the change in sensible energy, $\dot{U}_{sens}$, in response to changes in temperature and changes in the amount of latent energy associated with fusion, $\dot{U}_{sf}$. The thermal conductivity represents the ability of the porous medium to transmit heat in response to the temperature gradients (Equation 55).

4.2.1 Full Thermal

Table 9 summarizes the inputs required by the full thermal material model. Changes in sensible energy are characterized by volumetric heat capacity parameters for the unfrozen and frozen states, and the *in situ* volumetric water content. Thermal conductivity is a function of temperature, so it is indirectly a function of the portion of ice within the pore space (e.g., Andersland and Ladanyi, 2004).

Table 9. Parameters for the full thermal material model.

Parameter	Symbol	Unit
Thermal Conductivity function	$k(T)$	J/s/m/K (W/m/K)
Volume Heat Capacity: Unfrozen	C_p	J/m^3/K
Volume Heat Capacity: Frozen	C_p	J/m^3/K
Normalized Unfrozen Volumetric Water Content function	$\theta'_{uwc} = \frac{\theta_{uwc}}{n}(T)$	
In situ Volumetric Water Content	$\theta_w = n$	

The normalized unfrozen volumetric water content, θ'_{uwc}, is a function of temperature (Figure 6; e.g., Spaans and Baker, 1996; Flerchinger et al., 2006; Andersland and Ladanyi, 2004). This functional relationship controls the rate of change in the latent energy of fusion per degree temperature change, according to the second term on the left side of Equation 58. The normalized unfrozen volumetric water content acknowledges that water within a porous medium changes phase over a temperature range (Figure 6; see Section 4.2.4.1).

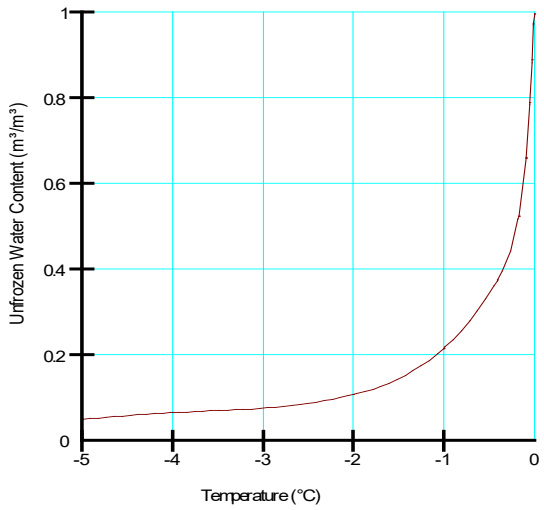

Figure 6. Example of an unfrozen water content versus temperature function.

4.2.2 Simplified Thermal

Table 10 summarizes the inputs required by the simplified thermal material model. The simplified thermal constitutive model assumes that all latent heat is released or adsorbed at a single phase change temperature. The change in volumetric ice content required by Equation 58 is assumed equal to the specified *in situ* volumetric water content.

Table 10. Parameters for the simplified thermal material model.

Parameter	Symbol	Unit
Thermal Conductivity: Unfrozen	k	J/s/m/K
Thermal Conductivity: Frozen	k	J/s/m/K
Volume Heat Capacity: Unfrozen	C_p	J/m^3/K
Volume Heat Capacity: Frozen	C_p	J/m^3/K
In situ Volumetric Water Content	θ_w	

The energy storage capacity for the simplified thermal model is defined in the same manner as the full thermal model: a volume heat capacity for both the frozen and unfrozen states. Similarly, conduction is characterized by specifying the thermal conductivity of the medium for the frozen and unfrozen states.

4.2.3 Coupled Convective

The coupled convective thermal material model can be used when the thermal properties of a material vary with volumetric water content. For example, this material model can be used when forced convection (or energy advection) is also being simulated. The fundamental difference between the coupled convective and full thermal material models is the assumption regarding volumetric water content. A full thermal material model assumes that the volumetric water content is constant

throughout the analysis, such that the frozen/unfrozen volume heat capacities are constant and the thermal conductivity is only a function of temperature. However, in a coupled heat and water transfer analysis, the volumetric water content within the domain is known, so the thermal properties can be defined as a function of the volumetric water content for the unfrozen state. The practical implication of these relationships is that the thermal properties can vary throughout the domain with changes in volumetric water content. Table 11 summarizes the inputs required by the coupled convective model.

Table 11. Parameters for the coupled convective material model.

Parameter	Symbol	Unit
Thermal Conductivity	$k' = k(\theta_w)$	J/s/m/K
Volume Heat Capacity	$C'_p = C_p(\theta_w)$	J/m^3/K
Normalized Unfrozen Volumetric Water Content function	$\theta'_{uwc} = \frac{\theta_{uwc}}{n}(T)$	

The coupled convective model adjusts the thermal conductivity and volumetric heat capacity if the temperature is below the phase change value (after Johansen, 1975). The porosity and total volumetric water content of the soil are known from the water transfer analysis. The unfrozen volumetric water content is calculated from the normalized function, θ'_{uwc}, at the current temperature as:

$$\theta_{uwc} = n\theta'_{uwc}(T) \qquad \text{Equation 61}$$

The volumetric ice content is the difference between the unfrozen and frozen water contents as:

$$\theta_{ice} = \theta_w - \theta_{uwc} \qquad \text{Equation 62}$$

The thermal conductivity of the soil in the partially frozen state, k_{pf}, is calculated via linear interpolation as:

$$k_{pf} = k' + \frac{\theta_{ice}}{\theta_w}\left[k_f - k'\right] \qquad \text{Equation 63}$$

where k' is the thermal conductivity at a given volumetric water content, and k_w is the thermal conductivity of liquid water. The thermal conductivity of the soil in a completely frozen state, k_f, is calculated as:

$$k_f = k_s^{(1-n)} k_{ice}^{(\theta_w)} \qquad \text{Equation 64}$$

where k_{ice} is the thermal conductivity of ice and the volumetric water content, θ_w, is equal to the volumetric ice content, θ_{ice}.

Finally, the thermal conductivity of the solids fraction, k_s, is calculated assuming the soil is unfrozen:

$$k_s = \left[\frac{k'}{(k_w)^{\theta_w}}\right]^{\left(\frac{1}{1-n}\right)} \quad \text{Equation 65}$$

The volumetric heat capacity of the soil in the partially or fully frozen state is calculated as:

$$C_{pf} = (1-n)C_s + \theta_{uwc}C_w + \theta_{ice}C_{ice} + \theta_a C_a \quad \text{Equation 66}$$

The volumetric heat capacity of the solids fraction, C_s, is calculated assuming the soil unfrozen as:

$$C_s = \frac{1}{1-n}\left(C'_p - \theta_w C_w - \theta_a C_a\right) \quad \text{Equation 67}$$

where C'_p is the volumetric heat capacity of a soil at a given water content, C_w is the volumetric heat capacity of water, C_a is the volumetric heat capacity of air, and θ_a is the volumetric air content.

4.2.4 Estimation Techniques

4.2.4.1 Normalized Unfrozen Volumetric Water Content Function

Various empirical or semi-empirical methods estimate the unfrozen volumetric water content function (e.g., Flerchinger et al., 2006; Spaans and Baker, 1996). GeoStudio provides a number of sample functions for the normalized unfrozen volumetric water content based on a range of soil particle size distributions (clay to gravel). These sample functions were generated by first calculating the change in water pressure for a shift in the freezing point temperature via the Clausius–Clapeyron thermodynamic equilibrium equation. The (negative) pore-water pressure at the freezing point temperature is then used to obtain the corresponding volumetric water content from the sample function referred to in Section 3.2.2.1. The volumetric water content is then normalized by the soil porosity and cross-plotted against the freezing point temperature to obtain a function similar to that shown in Figure 6.

4.2.4.2 Volumetric Heat Capacity, $C_p(\theta)$

The functional relationship between volumetric heat capacity and volumetric water content of an unfrozen soil, as required by the Coupled Convective Model (Section 4.2.3), can be estimated by (de Vries, 1975):

$$C_p = c_s\rho_s(1-n) + \theta_w C_w \quad \text{Equation 68}$$

where the specific heat capacity of the solids fraction, c_s, is defined by the user, and ρ_s is the solids density. The volumetric heat capacity of air is not included in Equation 68.

4.2.4.3 Thermal Conductivity, $k(T)$

The functional relationship between thermal conductivity and temperature required by the Full Thermal Model (Section 4.2.1) can be estimated as:

$$k = k_u + (MF)(k_f - k_u)$$ Equation 69

where k_u is the user defined unfrozen thermal conductivity, k_f is the user defined frozen thermal conductivity, and MF is a modifier factor uniquely defined for a range of freezing point temperatures. The modifier factor-temperature relationships are predefined for a range of particle size distributions based on measured data (e.g., Johansen, 1975).

4.2.4.4 Thermal Conductivity, $k(\theta)$

The functional relationship between thermal conductivity and volumetric water content of an unfrozen soil, as required by the Coupled Convective Model (Section 4.2.3), can be estimated by (Johansen, 1975; Farouki, 1981; Newman, 1995):

$$k' = (k_{sat} - k_{dry})\left(0.85 \log\left(\frac{\theta}{n}\right) + 1.0\right) + k_{dry}$$ Equation 70

where the thermal conductivity for the saturated condition, k_{sat}, is (refer to Equation 65):

$$k_{sat} = {k_w}^n\left[{k_s}^{(1-n)}\right]$$ Equation 71

where the mineral (solids) thermal conductivity is defined by the user. The thermal conductivity for the dry condition, k_{dry}, is given by:

$$k_{dry} = \frac{0.137\rho_d + 64.7}{2700 - 0.947\rho_d}$$ Equation 72

where the bulk dry density of a soil is estimated as:

$$\rho_d = \rho_s \frac{1-n}{1+n}$$ Equation 73

4.3 Boundary Conditions

4.3.1 Surface Energy Balance

The thermal response of a ground profile subject to climate conditions is generally considered a coupled soil-atmosphere process because the thermal energy flux (and concomitant ground surface temperatures) are dependent on water transfers across the ground surface, and the water transfers also depend on the ground surface temperatures. This coupled process can be modelled with the surface energy balance (SEB) boundary condition, which has the potential to reflect various ground surface conditions including bare, snow-covered, or vegetated ground. A boundary condition of this type can be used to simulate cyclic changes in ground temperatures for the purpose of exploring frost protection layers below trafficable surfaces, insulation configurations for foundations, or studying the preservation of frost in permafrost zones, mine wastes or soil covers.

4.3.1.1 Surface Energy Balance Equation

The SEB boundary condition represents a mathematical description of the energy transfers between the ground surface and the atmosphere. The amount of energy transmitted to the earth surface from the sun is the difference between the net solar (shortwave) and net terrestrial (longwave) radiation (i.e., net radiation). The net radiation drives several processes including evaporation (latent energy), warming or cooling of the air (sensible energy) and ground heat flux, and other smaller energy-consuming processes such as photosynthesis. The surface energy balance equation can be written for a heat transfer analysis as follows:

$$(q_{ns} - q_{nl}) = q_{sens} + q_{lat} + q_g \qquad \text{Equation 74}$$

where

q_{ns}	Net solar (shortwave) radiation
q_{nl}	Net terrestrial (longwave) radiation
$(q_{ns} - q_{nl})$	Net radiation
q_{sens}	Sensible heat flux
q_{lat}	Latent heat flux
q_g	Ground heat flux

The energy terms in this equation are fluxes, defined as the amount of energy that flows through a unit area per unit time. Equation 74 uses the sign convention of Sellers (1965) such that net radiation is positive downwards (toward the surface). As a result, latent and sensible heat fluxes are positive upwards (away from the surface), and ground heat flux is positive downward (into the ground). The energy balance equation states that all energy received at the earth's surface must be used to warm or cool the air above the ground surface, evaporate water, or warm or cool the ground profile.

The principal objective of conducting a TEMP/W analysis is to determine the thermal response of the ground subject to a given set of boundary conditions. Boundary conditions for heat transfer problems generally fall into two categories: 1) first type (i.e., temperature); or 2) second type (i.e., heat flux or heat transfer rate). The SEB boundary condition is calculated by solving the surface energy balance (Equation 74) as:

$$q_g = (q_{ns} - q_{nl}) - q_{sens} - q_{lat} \qquad \text{Equation 75}$$

As a result, the ground heat flux is calculated as the remaining energy flux after the other fluxes are satisfied.

4.3.1.1.1 Net Solar (Shortwave) Radiation

Most environmental processes operative at the surface of the earth are driven by solar radiation from the sun. On average, the earth receives around 118 MJ/m^2/day (0.0820 MJ/m^2/min) of solar radiation at the outer edge of the atmosphere (Allen et al., 1998). This quantity of solar radiation, termed the solar constant, occurs when the sun is directly overhead, so that the angle of incidence is zero. The local

intensity of the sun's radiation depends on the position of the sun relative to the position on earth. Consequently, the extraterrestrial radiation is a function of latitude, date, and time of day as follows:

$$q_{ext} = \frac{1}{\pi} G_{sc} d_r [\omega_s \sin\varphi \sin\delta + \cos\varphi \cos\delta \sin\omega_s] \quad \text{Equation 76}$$

where

q_{ext}	Extraterrestrial radiation
G_{sc}	Solar constant = 118 MJ/m^2/day
d_r	Inverse relative distance from earth to sun
ω_s	Sunset hour angle
φ	Latitude
δ	Solar declination

The inverse relative distance to the earth and the solar declination are given by:

$$d_r = 1 + 0.033 \cos\left(\frac{2\pi}{365} J\right) \quad \text{Equation 77}$$

and

$$\delta = 0.409 \sin\left(\frac{2\pi}{365} J - 1.39\right) \quad \text{Equation 78}$$

where J is the day of the year between 1 (January 1st) and 365 (December 31st) or 366 during a Leap Year. The solar declination represents the angle between the equatorial plane and a straight line joining the centres of the earth and sun.

The sunset hour angle, ω_s, is given by:

$$\omega_s = \cos^{-1}(-\tan\varphi \tan\delta) \quad \text{Equation 79}$$

Some of the extraterrestrial radiation is scattered, reflected, or absorbed by atmospheric gases, clouds, and dust before reaching earth's surface. The radiation reaching a horizontal plane on the earth's surface is the shortwave radiation. Cloud cover has a significant effect on shortwave radiation. Approximately 75% of extraterrestrial radiation reaches the earth's surface on a clear day (FAO, 1998). In contrast, only 25% reaches the earth's surface with extremely dense cloud cover. Ideally, the shortwave solar radiation at a specific site is measured; however, the Angstrom formula estimates the shortwave radiation by:

$$q_s = \left(a_s + b_s \frac{n}{N}\right) q_{ext} \quad \text{Equation 80}$$

where

q_s	Shortwave radiation
n	Actual duration of sunlight
N	Maximum possible duration of sunshine or daylight
q_{ext}	Extraterrestrial radiation
a_s, b_s	Regression constants
$a_s + b_s$	Fraction of q_{ext} reaching the earth on clear days ($n = N$)

The constants a_s and b_s are generally calibrated to measurements for a given site over some length of time such that long-term predictions of net radiation are consistent with site conditions. However, when data is not available, the values are assumed to be 0.25 and 0.5, respectively (FAO, 1998). The maximum number of daylight hours for a given day is determined by:

$$N = \frac{24}{\pi}\omega_s$$ Equation 81

The extraterrestrial and shortwave radiation estimated at a latitude of 52.17 degrees using Equation 76 and Equation 80, respectively, are illustrated in Figure 7. This estimation assumes a clear sky (i.e., $n = N$); consequently, the ratio of q_s/q_{ext} is constant (0.75) for every day of the year.

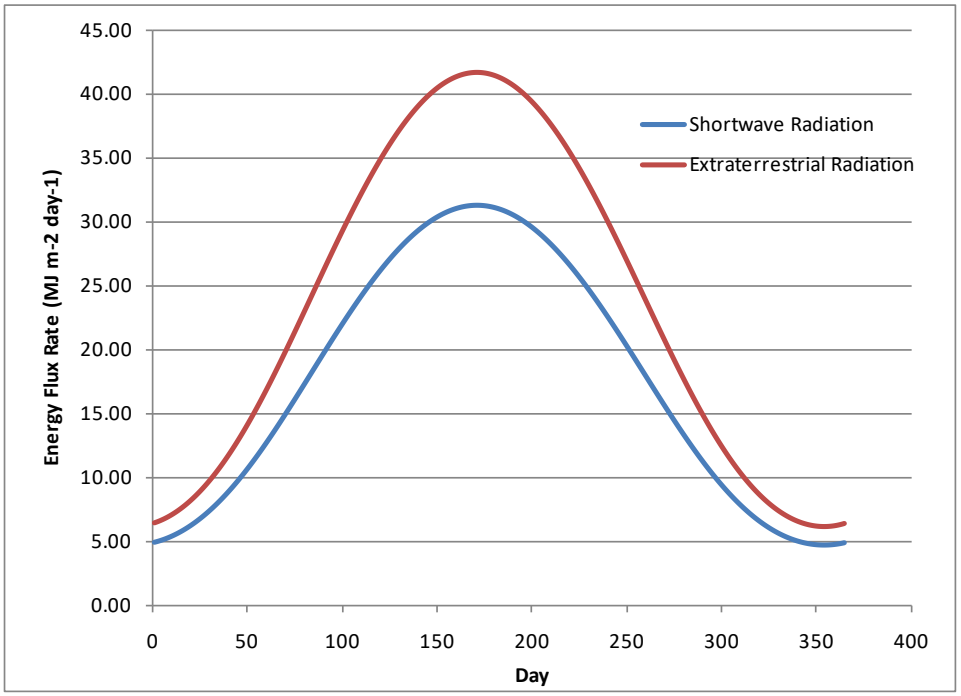

Figure 7. Estimated extraterrestrial and shortwave radiation at Latitude 52.17 degrees ($a_s = 0.25$; $b_s = 0.5$).

The earth's surface reflects a considerable amount of solar radiation back into the atmosphere. The reflected portion is known as the albedo, α, and it is dependent on the surface characteristics (among

other parameters). For example, the albedo of green vegetation is approximately 0.23 while that of fresh white snow is approximately 0.95 (FAO, 1998). The net solar radiation reaching the earth's surface (direct and diffuse), q_{ns}, also known as the short-wave radiation, is given as:

$$q_{ns} = (1 - \alpha)q_s \qquad \text{Equation 82}$$

where the net solar radiation is measured on a horizontal surface. The albedo is often based on field measurements or is estimated from literature values.

If the net solar radiation is measured directly, albedo can be used as a calibration coefficient. In that case, albedo incorporates the reflective property of the surface as well as a parameterization for cloud cover (as above) and angle of incidence/shadowing. The latter is important in hilly terrain in which some portion of the ground might be obstructed from direct sunlight. Dingman (2008) demonstrates procedures for incorporating all of these effects. A simple modification to Equation 82 for shadowing effects results in the expression:

$$q_{ns} = (1 - \alpha)q_s \times VF \qquad \text{Equation 83}$$

where VF is a view factor (which varies from 0 to 1) to account for angle of incidence and shadowing.

4.3.1.1.2 Net (Terrestrial) Longwave Radiation

A portion of the net solar radiation incident on the earth's surface is absorbed and converted into heat energy. Radiation is emitted from any heated surface due to the thermal energy of the surface matter. The rate of energy release per unit area of heated surface is the surface emissive power (Incropera et al., 2007). The upper limit to the emissive power, E_b, is achieved only by a surface called an ideal radiator (or blackbody), and is described by the Stefan-Boltzmann law:

$$E_b = \sigma {T_g}^4 \qquad \text{Equation 84}$$

where

σ Stefan-Boltzmann constant = 4.903×10^{-9} MJ/K^4/m^2/day = 5.67×10^{-8} W/m^2/K^4

T_g Absolute temperature of the (ground) surface

The energy emitted by a real surface, known as the long-wave radiation, E, is less than that of a blackbody at the same temperature and is given by:

$$E = \varepsilon_s \sigma {T_g}^4 \qquad \text{Equation 85}$$

where ε_s is the surface emissivity and is a value between 0.0 and 1.0. The surface emissivity provides a measure of how efficiently a surface emits energy relative to a blackbody. Sellers (1965) reports values of emissivity for dry and moist ground in the range of 0.9 to 0.98. Saito and Simunek (2009) present various approaches for computing emissivity as a function of water content for bare ground (i.e., no vegetation). TEMP/W assumes a value of 0.95 for estimating longwave radiation.

Some portion of the emitted long-wave radiation is lost into space. A portion is absorbed by water vapor and CO_2 in the atmosphere (including cloud cover). The longwave radiation adsorbed by the atmosphere increases its temperature and the atmosphere then radiates energy back toward the ground surface. Consequently, the earth's surface both emits and receives longwave radiation. The net longwave radiation is given by (van Bavel and Hillel, 1976):

$$q_{nl} = \varepsilon_s \sigma {T_g}^4 - \varepsilon_a \varepsilon_s \sigma {T_a}^4 \quad \text{Equation 86}$$

where ε_a and T_a are the air emissivity and air temperature, respectively. Expressions for air emissivity vary in the literature. Saito and Simunek (2009) presented air emissivity as a function of near-surface vapor pressure and/or air temperature. However, Saito and Simunek (2009) noted that most of the equations performed poorly for their test site. For simplicity, the following expression given by Idso (1981) is used:

$$\varepsilon_a = 0.70 + 5.95 \times 10^{-5} u_a e^{(1500/T_a)} \quad \text{Equation 87}$$

where the atmospheric vapor pressure, p_v^a, is calculated using the relationship proposed by Buck (1981) with an assumed relative humidity of 50%.

4.3.1.1.3 Sensible Heat Flux

Sensible heat flux is a convective heat transfer mechanism that derives its name from the ability to sense a temperature change caused by energy movement. Sensible heat transport occurs between a moving fluid (i.e., air) and a bounding surface (i.e., the ground) when the two are at different temperatures (Incropera et al., 2007). Convective heat transfer involves the combined processes of conduction (i.e., diffusion of heat through the still boundary layer next to the solid) and heat transfer by bulk fluid flow, a process referred to as heat advection. Positive sensible heat flux is upward or away from the surface and occurs when the ground surface is warmer than the air temperature. The rate equation is of the form:

$$q_{sens} = h\left(T_g - T_a\right) \quad \text{Equation 88}$$

where h is the heat transfer coefficient and the air temperature is usually measured at a reference height of 2 m (FAO, 1998).

The heat transfer coefficient attempts to accommodate a number of factors, including wind speed and surface roughness. Expressions for the heat transfer coefficient vary in the literature. Saito and Simunek (2009) present an equation for sensible heat flux that is in keeping with Dingman (2008). The equation is:

$$q_{sens} = C_a \frac{\left(T_g - T_a\right)}{r_a} \quad \text{Equation 89}$$

where r_a is the aerodynamic resistance to water vapor or heat flow from a soil surface to the atmosphere, and C_a is the volumetric heat capacity of air.

The aerodynamic resistance can be expressed as:

$$r_a = \frac{1}{uk^2}\left[ln\left(\frac{z_{ref} - d + z_h}{z_h}\right) + \mathrm{y}_h\right] \times \left[ln\left(\frac{z_{ref} - d + z_m}{z_m}\right) + \mathrm{y}_m\right] \quad \text{Equation 90}$$

where

u	Wind speed
k	von Karman's constant = 0.41
z_{ref}	Reference height for measurements (typically 1.5 m)
d	Zero-plane displacement height
$z_{h,m}$	Surface roughness height for heat and momentum flux, respectively
$\mathrm{y}_{h,m}$	Atmospheric stability correction factor for momentum and heat flux

The zero-plane displacement height, d, is generally assumed to be 2/3 the vegetation height, while the surface roughness values, z_h and z_m, are assumed to be 0.1 and 0.123 times the vegetation height, respectively (Dingman, 2008; Saito and Simunek, 2009). The typical surface roughness height for bare ground is 0.001 m, with a zero-plane displacement height of zero. It is generally assumed that the resistance to momentum and heat flow are the same, so the heat and momentum flux surface roughness values are assumed equivalent (i.e., z_h = z_m).

The atmospheric stability correction factors for momentum and heat flux are assumed equal. In general, determination of the factors requires an iterative solution. Saito and Simunek (2009) found that a simplified correction, which was developed by Koivusalo et al. (2001), performed equally as well. The correction requires the calculation of the Richardson number, R_i, as:

$$R_i = \frac{g\left(z_{ref}\right)\left(T_a - T_g\right)}{\left(T_a\right)u^2} \quad \text{Equation 91}$$

The stability correction for stable and unstable conditions is:

$$\mathrm{y} = (1 - 10R_i)^{-1} \text{ for } \mathrm{R_i} < 0$$
$$\mathrm{y} = (1 + 10R_i)^{-1} \text{ for } \mathrm{R_i} > 0 \quad \text{Equation 92}$$

The aerodynamic resistance is calculated by setting y = 0 in Equation 90, which yields the neutral aerodynamic resistance, r_{aa}. The aerodynamic resistance is then calculated using the non-zero value of the stability correction from Equation 92:

$$r_a = r_{aa}\mathrm{y} \quad \text{Equation 93}$$

4.3.1.1.4 Latent heat flux

Latent heat refers to the amount of energy released or absorbed by water during a change of state that occurs without changing its temperature. The term latent infers that energy is being stored in the water molecules and can be released during condensation. The latent heat of vaporization of water is 2.45 MJ/kg at 20 °C; thus, it takes 2.45 MJ of energy to evaporate 1 kg of water, which is equivalent to 1 mm

of water over a square meter of area given a water density of 1000 kg/m^3. The latent heat flux in Equation 74 is given by:

$$q_{lat} = AE\left(\frac{1}{1000}\right)\rho_w h_{sf} \quad \text{Equation 94}$$

where AE is the actual evapotranspiration. The actual evaporation can be established using two options in TEMP/W: 1) user-defined; and, 2) 'From Water Transfer Analysis'. The first option requires the definition of an AE verses time function using measured or estimated data. The second option requires a SEEP/W analysis with a land-climate interaction boundary condition.

4.3.1.1.5 Accommodating the Snowpack

The surface energy balance equation can be re-written to accommodate the presence of snow during the winter months as:

$$q_{snow} = q_g = (q_{ns} - q_{nl}) - q_{sens} - q_{lat} \quad \text{Equation 95}$$

where the energy flux through the snow, q_{snow}, is assumed equal to the ground heat flux. This assumption requires that the snow has no capacity to store energy. For implementation purposes, Equation 95 is recast as:

$$0 = -(q_{ns} - q_{nl}) + q_{sens} + q_{lat} + q_{snow} \quad \text{Equation 96}$$

The sensible heat flux (Equation 89) and net longwave radiation (Equation 86) are calculated using the temperature at the top of the snow (not the ground temperature). The energy flux through the snow is given by:

$$q_{snow} = -k_{snow}\frac{(T_g - T_{snow})}{h_{snow}} \quad \text{Equation 97}$$

where

k_{snow}	Thermal conductivity of snow
T_{snow}	Temperature at snow surface
T_g	Temperature at ground surface
h_{snow}	Depth of snow

The implicit assumption of this approach is that the specific heat capacity (i.e., the ability to store or release energy) of the snow pack is negligible relative to the energy flux through the snow. A downward heat flux through the snow is considered positive as this implies warming of the ground. Latent heat flux is assumed to be zero during the winter.

4.3.1.2 Inputs

Table 12 summarizes the most rigorous inputs for the SEB boundary condition associated with each of the energy flux components. The net radiation energy flux drives the other processes and is naturally a principal input for the SEB boundary condition. To calculate sensible heat flux, both the air temperature

and wind speed functions are required. The snow depth and vegetation height functions are optional. TEMP/W assumes bare ground conditions if the vegetation depth function is not defined. Similarly, an evaporative flux of zero is assumed if the function is not defined.

Table 12. Inputs for the surface energy balance boundary condition.

Energy Flux	Inputs
Net radiation flux	Net radiation flux versus time (i.e., measured)
Sensible heat flux	Air temperature versus time Wind speed versus time Vegetation height versus time (optional)
Latent heat flux	Actual evaporation versus time or SEEP/W results
Ground heat flux	Snow depth versus time (optional) Snow pack thermal conductivity

The net radiation flux may not be available for some sites. As such, the user can elect to input the incoming solar radiation flux (Table 13). There are two options: 1) measured solar radiation flux data; or, 2) estimated solar radiation flux given a user-defined latitude (Equation 76). In either case, an albedo function must be defined such that the net solar radiation can be calculated according to Equation 82. The net longwave radiation is computed with Equation 86 and the net radiation is calculated as the difference between net shortwave and net longwave radiation (Equation 74).

Table 13. Alternative inputs for the SEB boundary condition if net radiation flux is not measured.

Alternative	Equation	Inputs
Measured solar radiation	--	• Measured solar radiation flux versus time • Albedo versus time
Estimated solar radiation	Equation 80	• Estimated solar radiation flux versus time • Albedo versus time

4.3.2 n-Factor

The n-Factor boundary condition uses the ratio of the ground surface and air freeze/thaw indexes to calculate the simulated ground surface temperature. Each index is computed as the integral (or area) of the temperature versus time function that lies above (thawing) or below (freezing) the phase change temperature (T_0), such that

$$n = \frac{I_g}{I_a} = \frac{\int_0^{t_g}(T_0 - T_g)\mathrm{d}t}{\int_0^{t_a}(T_0 - T_a)\mathrm{d}t} \qquad \text{Equation 98}$$

where t_g, t_a are the durations of the ground surface and air freeze/thaw seasons, respectively; and T_g, T_a are the ground surface and air temperatures, respectively. The mean ground surface temperature, for the freeze or thaw season, can therefore be computed as

$$\overline{T_g} = n(\overline{T_a} - T_0)\frac{t_a}{t_s} + T_0 \qquad \text{Equation 99}$$

where $\overline{T_a}$ is the mean air temperature for the corresponding season. The ground surface temperature at an instant in time can be computed from the air temperature by simplifying the equation as follows:

$$T_g = n(T_a - T_0) + T_0 \qquad \text{Equation 100}$$

4.3.2.1 Inputs

The inputs for the n-Factor boundary condition are:

- Air temperature as a function of time
- n-Factor for thawing conditions
- n-Factor for freezing conditions

The magnitude of freezing and thawing n-Factors depends on the climatic conditions, as well as on the material type at the ground surface.

4.3.3 Convective Surface and Thermosyphon

The Convective Surface and Thermosyphon boundary conditions both apply Newton's Law of Cooling to calculate a heat flux. The heat flux is then: a) numerically integrated over a surface area to apportion an energy flux to the nodes associated with the surface (second-type); or b) multiplied by a user entered convective surface area (e.g., perimeter of pipe x 1 unit length into page) to obtain an energy rate applied to a single node.

4.3.3.1 Newton's Law of Cooling

Convective heat transport is assumed to occur between a moving fluid and a bounding surface when the two are at different temperatures (Incropera et. al, 2007). Convective heat transfer involves the combined processes of conduction (i.e., diffusion of heat through the still boundary layer next to the solid surface) and heat transfer by bulk fluid flow, referred to as heat advection. The rate equation describing convective heat transfer (Newton's Law of Cooling) is:

$$q_{sur} = h(T_{sur} - T_\infty) \qquad \text{Equation 101}$$

where q_{sur} is the surface heat flux due to convection, h is the convection heat transfer coefficient, T_{sur} temperature of the bounding surface, and T_∞ the temperature of the fluid outside the thermal boundary layer. The thermal boundary layer develops in response to the velocity boundary layer – the zone in which there are high velocity gradients. A positive heat flux indicates energy transfer from a warm surface to a cooler fluid.

4.3.3.2 Inputs: Convective Surface

The inputs for the convective surface boundary condition are:

- Fluid temperature as a function of time
- Convective heat transfer coefficient, h, versus time
- Convective surface area (only if the boundary condition is applied to a point)

A convective surface boundary condition can be used to simulate artificial ground freezing or other processes that involve fluid flow over a surface. For example, Andersland and Ladanyi (2004) explore the use of a convective surface boundary condition to represent the surface energy balance at the ground surface. For cases involving internal flow through a conduit, heat transfer occurs by conduction through the conduit wall and then by convective heat transfer from the inside wall of the conduit into the flowing fluid. In a numerical analysis, however, the convection heat transfer coefficient embodies the conditions within the boundary layer, as well as the heat transfer characteristics and geometry of the conduit. Thus, the boundary condition is applied at the outside conduit wall.

The area of the convective surface is calculated via numerical integration if the boundary condition is applied to an edge comprised of line segments. In contrast, application of the boundary condition to a point, which inherently has no area, requires specification of the surface perimeter. The surface perimeter, which is equal to the outside circumference of a pipe in ground freezing applications, is multiplied by the element thickness to obtain the surface area.

Incropera et al. (2007) describes the difficulties in defining the convection coefficient a priori. In addition to depending on numerous fluid properties such as density, viscosity, thermal conductivity, and specific heat capacity, the convection coefficient depends on the surface geometry and flow conditions. The convection coefficient can be obtained by solving the boundary layer equations for simple flow situations. The more practical approach involves calculation of a Nusselt number, Nu, and subsequent calculation of a convection heat transfer coefficient from the functional relationship:

$$\mathrm{Nu} = \frac{hL}{k_f} \qquad \text{Equation 102}$$

where k_f is the thermal conductivity of the fluid and L is a characteristic length (e.g., hydraulic diameter = outer diameter – inner diameter). The Nusselt number can vary with time in response to the flow conditions (i.e., laminar or turbulent), temperature gradients, and other factors; consequently, the convection heat transfer coefficient is input as a function of time. The convection heat transfer coefficient for brine freezing applications typically ranges between 25 and 75 W/m^2/°C.

4.3.3.3 Inputs: Thermosyphon

The inputs for the thermosyphon boundary condition are:

- Air temperature as a function of time
- Wind speed with time
- Convective heat transfer coefficient versus wind speed
- Surface perimeter (only if the boundary condition is applied to a point)
- Maximum operating air temperature
- Minimum temperature difference for vaporization

A common application of a thermosyphon is to maintain frozen conditions beneath surface infrastructure, such as a roadway, constructed over permafrost. Thermosyphons transfer heat from the

ground if the air temperature moving past the condenser is less than ground temperature. Thermosyphons comprise an evaporator section installed in the ground and a condenser section exposed to atmospheric conditions.

The overall heat conductance of a thermosyphon is defined as the heat rate extracted from the device divided by the temperature difference between the evaporator and air flowing past the condenser. Haynes and Zarling (1988), for example, measured overall heat conductance of a thermosyphon by placing the condenser in a wind tunnel maintained at constant temperature. The evaporator was also maintained at a constant temperature via a heated water bath. The overall heat conductance was measured at various wind speeds and the data described by empirical relationships of the form:

$$Heat\ transfer\ conductance = A + B(u^n) \qquad \text{Equation 103}$$

where A and B are coefficients, n an exponent, and u the fluid (wind) velocity. The convection heat transfer coefficient can be calculated by dividing the overall heat conductance by the total area of the evaporator, and input as a function of wind speed.

Heat transfer through the thermosyphon ceases if: a) the air temperature is greater than the ground temperature; b) the air temperature exceeds a user specified maximum operating value; or, c) the temperature difference between the air and outside wall of the evaporator (i.e., ground) is not great enough to cause vaporization of the fluid (e.g., $C0_2$ or Anhydrous Ammonia).

Thermosyphons are most commonly applied to circular openings (i.e., edges of elements) or to a point (i.e., node) in a 2D analysis. The evaporator of the thermosyphon is viewed in cross-section when the boundary condition is applied in this manner. Similar to the convective surface boundary condition, the surface area of the evaporator section is calculated via numerical integration when the boundary condition is applied to an edge comprising line segments. In contrast, application of the boundary condition to a point, which inherently has no area, requires specification of the surface perimeter. The surface perimeter, which is equal to the outside circumference of the evaporator, is multiplied by the element thickness to obtain the surface area of the evaporator. The thermosyphon boundary condition can also be applied to a line in an axisymmetric analysis to model a single vertical thermosyphon.

4.3.4 Estimation Techniques

4.3.4.1 Sinusoidal Distribution of Cumulative Daily Radiation

Cumulative daily net radiation and cumulative daily shortwave radiation are the time-integrated values of the radiation flux (e.g., Figure 7). The cumulative daily radiation is often reported as an energy flux; however, it is more appropriate to consider this measurement as the total quantity of energy over a unit area of the ground surface in one day. The user has the option to apply the cumulative daily radiation flux directly, which is equivalent to assuming that the flux is constant over the day. There is also the option to distribute sinusoidally over each day. The radiation flux at any instant during the day is then estimated from the cumulative value as:

$$(q_{ns} - q_{nl}) = Asin\theta \qquad \text{Equation 104}$$

where

$A =$ Normalized Amplitude = $(\pi/2N)$

$\theta =$ Normalized time $(0 < \theta < \pi)$

Figure 8 presents the incoming solar radiation flux associated with a sinusoidal distribution of cumulative daily solar radiation. Sunrise and sunset are assumed to occur symmetrically around noon based on the maximum number of daylight hours for a given day (Equation 81). Net radiation is generally non-zero before and after sunrise and sunset, respectively, because the ground continues to emit net longwave radiation. However, the option to distribute a cumulative daily net radiation value assumes that the net radiation is zero before sunrise and after sunset.

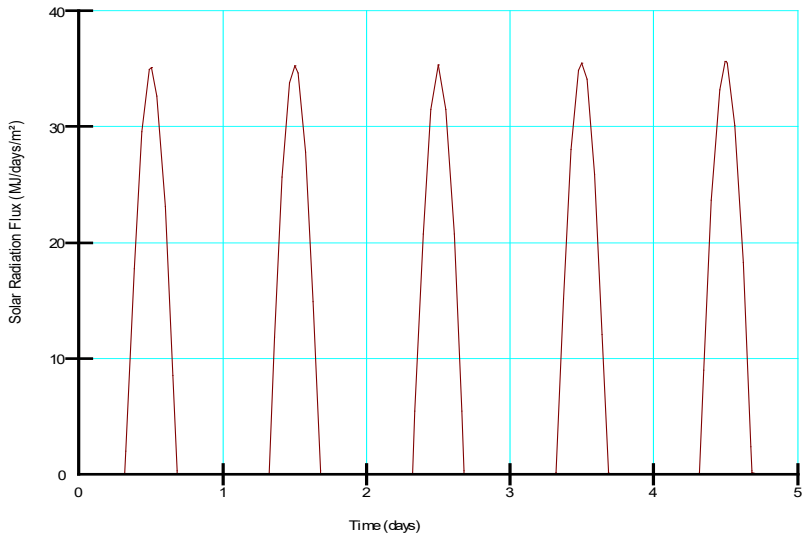

Figure 8. Example of sinusoidal radiation flux.

5 Air Transfer

AIR/W (or AIR3D) is a finite element program for simulating air transfer. Although it can be a standalone product, the true power in the AIR/W formulation lies with the increased functionality it provides when combined with other GeoStudio products. For example, AIR/W can be coupled with TEMP/W to model forced convection heat transfer, with CTRAN/W to model gas transfer via advection, or with SEEP/W to model coupled air-water systems. Section 5.1 summarizes the air transfer and storage processes included in the formulation. Section 5.2 describes the constitutive models available to characterize the air transfer and storage processes of the medium. Section 5.3 describes the boundary conditions that are unique to this product beyond the basic FEM boundary conditions described in Section I.7.

5.1 Theory

The AIR/W formulation is based on the mass conservation statement (Equation 1 in Section 3.1). The rate of change in the mass of air stored in the REV is given by:

$$\dot{M}_g = \dot{M}_a + \dot{M}_d + \dot{M}_v \qquad \text{Equation 105}$$

The subscript g has been used denote pore-gas, which comprises dry air (a), dissolved dry air (d), and water vapor (v). The mass of dissolved air and water vapor are assumed negligible and are omitted from the AIR/W formulation. The rate of change in the mass of dry air within the control volume is calculated with the ideal gas law (see Equation 5):

$$\dot{M}_a = \frac{\partial M_a}{\partial t} = \frac{M}{R}\left[\frac{\theta_a}{T}\frac{\partial u_a}{\partial t} + \frac{\bar{u}_a}{T}\frac{\partial \theta_a}{\partial t} + \bar{u}_a\theta_a\frac{\partial}{\partial t}\left(\frac{1}{T}\right)\right]dx\,dy\,dz \qquad \text{Equation 106}$$

where M is the molar mass, R is the gas constant, θ_a is the volumetric air content, u_a is pore air pressure, and $\bar{u}_a$ absolute air pressure. The temporal derivative of the volumetric air content is equal to the negative of the temporal derivative of the volumetric water content:

$$\frac{\partial \theta_a}{\partial t} = -\frac{\partial \theta_w}{\partial t} = -\left(m_w\frac{\partial u_a}{\partial t} - m_w\frac{\partial u_w}{\partial t}\right) \qquad \text{Equation 107}$$

where m_w is the slope of the volumetric water content function.

The air mass flow rate in response to mechanical energy gradients follows a similar form as Darcy's Law for variable density liquid water flow:

$$\dot{m}_a = \rho_a q_a dxdz = \frac{-k_a}{g}\left(\frac{\partial u_a}{\partial y} + \rho_a g\frac{\partial y}{\partial y}\right)dxdz \qquad \text{Equation 108}$$

where q_a is the volumetric air flux and k_a is the (dry) air hydraulic conductivity. Substitution and expansion of Equation 106 and Equation 108 into the conservation statement and division by the volume of the REV gives:

$$\rho_a\left[\left(\frac{\theta_a}{\bar{u}_a} - m_w\right)\frac{\partial u_a}{\partial t} + m_w\frac{\partial u_w}{\partial t} + T\theta_a\frac{\partial}{\partial t}\left(\frac{1}{T}\right)\right] = \frac{\partial}{\partial y}\left[\frac{k_a}{g}\left(\frac{\partial u_a}{\partial y} + \rho_a g\frac{\partial y}{\partial y}\right)\right] \qquad \text{Equation 109}$$

Equation 109 can be simplified by assuming isothermal conditions with constant water content (i.e., single-phase air transfer):

$$\rho_a\frac{\theta_a}{\bar{u}_a} = \frac{\partial}{\partial y}\left[\frac{k_a}{g}\left(\frac{\partial u_a}{\partial y} + \rho_a g\frac{\partial y}{\partial y}\right)\right] \qquad \text{Equation 110}$$

Table 14 summarizes the physical processes included in the partial differential equation solved by AIR/W. The left side of Equation 109 includes the rate of change in the mass of air due to changes in air density and air content. The formulation implicitly includes the effect of changes in pore-air pressure

and temperature on storage via the ideal gas law. Changes in air content are linked to changes in water content and, therefore, pore-water pressure. The right side of Equation 109 includes air transfer in response to gradients in pore-air pressure and density.

Table 14. Summary of the physical processes included in the AIR/W formulation.

Physical Process	GeoStudio Products
Storage: air compressibility	AIR/W
Storage: soil structure compressibility	AIR/W + SEEP/W
Storage: matric suction changes due to pore-water pressure changes	AIR/W + SEEP/W
Storage: matric suction changes due to pore-air pressure changes	AIR/W + SEEP/W
Storage: air density changes due to temperature changes	AIR/W + TEMP/W
Flow: pressure-driven (isothermal)	AIR/W
Flow: gravity-driven	AIR/W
Flow: density-driven via thermal effects (free convection)	AIR/W + TEMP/W

The key elements of the AIR/W formulation are as follows:

- The default physical processes in AIR/W include pressure and gravity-driven flow and storage changes due to changes in air pressure.
- Thermal effects on air density, which exerts control on both storage and flow, are included by coupling AIR/W and TEMP/W. This is achieved by selecting the option for free convection: thermal effects.
- AIR/W can be coupled with SEEP/W to simultaneously model water transfer and its effect on air transfer and storage (and vice versa). This is achieved by solving air and water transfer on the same domain. Thermal effects can also be included with this type of analysis (AIR/W + SEEP/W + TEMP/W).

5.2 Material Models

5.2.1 Single Phase

Single phase pore-air transfer through porous media can be modelled assuming that the volumetric air content (and water content) are constant. This material model can be applied to AIR/W and coupled AIR/W-TEMP/W analyses, but not for coupled AIR/W-SEEP/W analyses. The parameters required for this material model are presented in Table 15. Air conductivity is assumed to be isotropic for this material model. Changes in air storage are a function of the air content and air density, with the latter calculated internally according to the ideal gas law.

Table 15. Parameters for the single-phase material model.

Parameter	Symbol	Unit
Air Conductivity	k_a	m/s
Volumetric Air Content	θ_a	

5.2.2 Dual Phase

The dual-phase material model is required for coupled AIR/W-SEEP/W analyses. The parameters required for this material model are presented in Table 16. Air conductivity governs the resistance to flow and is entered as a function of saturation. The air content is no longer an input because it is determined directly from the volumetric water content function used in the SEEP/W water transfer analysis. As in the single-phase material model, air density is calculated according to the ideal gas law given the air pressure and temperature.

Table 16. Parameters for the single-phase material model.

Parameter	Symbol	Unit
Air Conductivity Function	$k_a(S)$	m/s

5.2.3 Estimation Techniques

5.2.3.1 Air Conductivity Function

GeoStudio uses the closed-form equation presented by Ba-Te et al. (2005) to estimate the air conductivity function. The equation is given as:

$$k_a = k_{dry}(1-S)^{1/2}\left(1-S^{1/q}\right)^{2q} \qquad \text{Equation 111}$$

where k_{dry} is the air conductivity of the dry soil, S is the saturation of the soil, and q is a curve fitting parameter related to pore-size distribution (assumed to be 2.9 after Fredlund et al., 2012).

5.3 Boundary Conditions

The conventional first and second type boundary conditions as described in Section 0 can be used within an air flow analysis. However, simulating the effect of atmospheric air pressure on the ground surface requires a unique boundary condition.

5.3.1 Barometric Air Pressure

The barometric air pressure boundary condition is used to simulate the variability in atmospheric air pressure along a sloping ground surface. The air pressure, u_{a_y}, at an arbitrary elevation, y, is calculated according to the barometric formula:

$$u_{a_y} = \bar{u}_{a_0} e^{\left(\frac{-Mg}{RT_a}(y-y_0)\right)} - \bar{u}_{a_{NIST}}$$ Equation 112

where $\bar{u}_{a_0}$ is the atmospheric air pressure measured at the elevation y_0 and air temperature T_a, and $\bar{u}_{a_{NIST}}$ the standard atmospheric pressure at sea level (i.e. 101.325 kPa). Absolute pressure is zero-referenced against a perfect vacuum while gauge pressure is zero-referenced against the ambient air pressure. Absolute pressure is therefore equal to atmospheric pressure plus gauge pressure. Exposure of an absolute pressure measurement device to the atmosphere allows for measurement of barometric air pressure, which naturally corresponds to a gauge pressure of zero. The air pressure u_{a_y} in Equation 112 must therefore be thought of as a differential pressure; that is, the air pressure measured by a device that is zero referenced against standard atmospheric pressure at sea level.

6 Solute and Gas Transfer

CTRAN/W (or CTRAN3D) is a finite element program for simulating the transport of a dissolved constituent or gas through porous media. Typical applications for CTRAN/W include dissolved solute or gas transport through regional or local groundwater flow systems, or oxygen transport through air and water within unsaturated mine waste. Section 6.1 summarizes the solute and gas transfer and storage processes included in the CTRAN/W formulation. Section 6.2 describes the constitutive models available to characterize the solute and gas transfer and storage processes, and Section 6.3 describes the boundary conditions unique to this product.

6.1 Theory

The governing equations for solute and gas transfer in CTRAN/W are based on the law of mass conservation in the same manner as the water (Section 3.1) and air (Section 5.1) transfer formulations.

6.1.1 Solute Transfer

The rate of change in the mass of solute stored in a control volume is given by:

$$\dot{M}_{st} = \dot{M}_{dp} + \dot{M}_{ap} \qquad \text{Equation 113}$$

The subscript dp and ap have been used to denote dissolved and adsorbed phases. This equation can be expanded to:

$$\dot{M}_{st} = \frac{\partial}{\partial t}(C\theta_w + \rho_d S^*)dx\,dy\,dz \qquad \text{Equation 114}$$

where C is the mass concentration in the dissolved phase, ρ_d is the dry bulk density of the soil (M_s/V_t), and S^* is the quantity of mass (M) sorbed per mass of solids (M_s).

First order kinematic reactions such as radioactive decay, biodegradation, and hydrolysis result in mass consumption within the control volume. Thus, a sink term is now included in the conservation statement $(\dot{M}_S)$ to represent the first order reaction processes. The rate of change in the solute mass due to decay, $\dot{M}_\lambda$, is given by:

$$\dot{M}_\lambda = -\lambda\left(\theta_w C + \rho_d S^*\right) dx\,dy\,dz = -\dot{M}_S \qquad \text{Equation 115}$$

where λ is the reaction constant.

The mass flow rate in response to concentration gradients, $\dot{m}_D$, can be evaluated according to Fick's Law:

$$\boldsymbol{\dot{m}_D = J_D dxdz = -D_d^* \theta_w \frac{\partial C}{\partial y} dxdz} \qquad \text{Equation 116}$$

where J_D is the diffusion mass flux and D_d^* is the bulk diffusion coefficient, which accounts for the effects of tortuosity. The bulk diffusion coefficient can be replaced by a coefficient of hydrodynamic dispersion that incorporates the combined effects of diffusion and mechanical dispersion:

$$D = D' + D_d^* \qquad \text{Equation 117}$$

where D' is the coefficient of mechanical dispersion, which can be expanded to give:

$$D = \alpha v_w + D_d^* \qquad \text{Equation 118}$$

where α is the dispersivity of the medium and v_w is the groundwater velocity. It is important to note that mechanical dispersion is represented as a tensor rather than a scalar in multi-dimensional problems while the bulk diffusion coefficient is represented as a scalar.

Advection solute transport is mass transport due to the flow of water in which the mass is dissolved. The direction and rate of transport coincide with the groundwater flow. The groundwater flux is described by the Darcy Equation. The advective mass flow rate, $\dot{m}_A$, is given by:

$$\dot{m}_A = J_A dxdz = (\theta_w C) v_w dxdz = C q_w dxdz \qquad \text{Equation 119}$$

where J_A is the advective mass flux, $(\theta_w C)$ is the amount of dissolved mass relative to the control volume, and q_w is the water flux, which is related to the linear groundwater velocity by q_w/θ_w.

Substitution and expansion of the foregoing rate equations into the conservation statement and division by the dimensions of the control volume gives the divergence form of the solute transfer equation:

$$\left(\theta_w + \rho_d \frac{\partial S^*}{\partial C}\right)\frac{\partial C}{\partial t} + C\frac{\partial \theta_w}{\partial t} = \frac{\partial}{\partial y}\left[D\theta_w \frac{\partial C}{\partial y} - C q_w\right] - \lambda(\theta_w C + \rho_d S) \qquad \text{Equation 120}$$

where $\partial S^*/\partial C$ is the equilibrium sorption isotherm or the adsorption coefficient (K_d).

Table 17 summarizes the physical processes included in the partial differential equation solved by CTRAN/W for solute transfer. The left side of Equation 120 includes rates of mass change in response to concentration changes, adsorption, and water content changes. The right side of Equation 120 includes solute transfer via diffusion and advection-dispersion, along with the first order reaction losses from the dissolved and adsorbed mass.

Table 17. Summary of the physical processes included in the CTRAN/W solute transfer formulation.

Physical Process	GeoStudio Products
Storage: concentration changes	CTRAN/W + SEEP/W
Storage: water content changes	CTRAN/W + SEEP/W
Storage: adsorption	CTRAN/W + SEEP/W
Storage: decay of dissolved and adsorbed mass	CTRAN/W + SEEP/W
Flow: diffusion	CTRAN/W + SEEP/W

Flow: advection-dispersion with water transfer	CTRAN/W + SEEP/W

The key elements of the CTRAN/W solute transfer formulation are as follows:

- The default simulated physical processes include storage changes due to variation in concentration, adsorption, decay, and diffusive transport. Advection-dispersion is an optional physical process.
- A SEEP/W analysis must always be defined for a solute transfer analysis because of the water content term in Equation 120.
- Changes in storage due to changes in water content due to vaporization or condensation are only considered if the coupled SEEP/W analysis includes the physical process of isothermal and/or thermal vapor flow.

6.1.2 Gas Transfer

The gas transfer equation is derived in a similar manner as the solute transfer equation (Section 6.1.1). CTRAN/W considers gas movement in the gas phase and the aqueous phase. The convective form of the gas transport equation is given as:

$$\theta_{eq}\frac{\partial C_{gp}}{\partial t} = \frac{\partial}{\partial y}\left[(D_a\theta_a + D_w H\theta_w)\frac{\partial C_{gp}}{\partial y}\right] - q_a\frac{\partial C_{gp}}{\partial y} - Hq_w\frac{\partial C_{gp}}{\partial y} - K_r^*\theta_{eq}C_{gp} - \lambda\theta_{eq}C_{gp} \quad \text{Equation 121}$$

where C_{gp} is concentration in the gas phase, D_a and D_w are the coefficients of hydrodynamic dispersion for gas transport in the gas and aqueous phases, respectively, and H is the dimensionless form of Henry's equilibrium constant (i.e., C_{dp}/C_{gp} where C_{dp} is the gas concentration in the dissolved or aqueous phase). The air and water fluxes are q_a and q_w, respectively, K_r^* is the bulk reaction rate coefficient for irreversible first order reaction processes such as oxidation, and λ is the decay constant for radioactive decay or some reaction rate coefficient for biodegradation or hydrolysis.

The equivalent diffusion porosity, θ_{eq}, was defined by Aubertin et al. (2000) as:

$$\theta_{eq} = \theta_a + H\theta_w \quad \text{Equation 122}$$

The coefficients of hydrodynamic dispersion comprise both the coefficient of mechanical dispersion $(D' = \alpha v)$ and bulk diffusion coefficient (D_d^*) for each phase such that:

$$D_w = \alpha_w v_w + D_{dw}^* \quad \text{Equation 123}$$

and

$$D_a = \alpha_a v_a + D_{da}^* \quad \text{Equation 124}$$

Table 18 summarizes the physical processes included in the partial differential equation solved by CTRAN/W for gas transfer. The left side of Equation 121 includes rates of mass change in response to concentration changes. The right side includes gas transfer via diffusion in the gas and dissolved phases

and advection-dispersion in the gas and dissolved phases. The formulation also includes the decay of mass within the gaseous and aqueous phases, as well as first order reaction processes (i.e., consumption).

Table 18. Summary of the physical processes included in the CTRAN/W gas transfer formulation.

Physical Process	GeoStudio Products
Storage: concentration changes	CTRAN/W + SEEP/W
Storage: decay of gas in free and dissolved phases	CTRAN/W + SEEP/W
Storage: consumption in the free and dissolved phases	CTRAN/W + SEEP/W
Flow: diffusion in the free and dissolved phases	CTRAN/W + SEEP/W
Flow: advection-dispersion with water transfer	CTRAN/W + SEEP/W
Flow: advection-dispersion with air transfer	CTRAN/W + SEEP/W + AIR/W

The key elements of the CTRAN/W gas transfer formulation are as follows:

- The default simulated physical processes include concentration changes via decay or reaction processes, and diffusive transport. Advection-dispersion with water and/or air transfer is an optional physical process.
- A SEEP/W analysis must always be defined for a gas transfer analysis because of the equivalent diffusion porosity term in Equation 121.
- The concentration in the gas and dissolved phases is assumed to be in equilibrium.

6.2 Material Models

6.2.1 Solute Transfer

There is only one material model available in a CTRAN/W analysis. The parameters required for this material model are presented in Table 19. The bulk diffusion coefficient is defined as a function of water content and the adsorption is defined as a function of concentration. The first order reaction coefficient is calculated internally from the specified reaction half-life (Equation 120). The longitudinal and transverse dispersivity inputs are only visible if advection-dispersion is included in the analysis.

Table 19. Parameters for a solute transfer material model.

Parameter	Symbol	Unit
Bulk Diffusion Coefficient function	$D(\theta_w)$	m^2/s
Adsorption function	$K_d(C)$	Mg/Mg
Decay Half-Life	$t_{1/2}$	s
Dry Density	ρ_d	Mg/m^3
Longitudinal Dispersivity	α_L	m

Transverse Dispersivity	α_T	m

6.2.2 Gas Transfer

There is only one material model available for a CTRAN/W gas transfer analysis. The parameters required for this material model are presented in Table 20. The bulk diffusion coefficients for the gas and water phases are defined as a function of water content. The bulk reaction rate coefficient is also defined as a function of water content. As for a solute transfer analysis, the decay half-life is used internally to calculate the decay constant in Equation 121. The longitudinal and transverse dispersivity inputs are only visible when advection-dispersion is included in the analysis.

Table 20. Parameters for a gas transfer material model.

Parameter	Symbol	Unit
Bulk Diffusion Coefficient function in Gas Phase	$D^*_{da}(\theta_w)$	m^2/s
Bulk Diffusion Coefficient function in Water Phase	$D^*_{dw}(\theta_w)$	m^2/s
Bulk Reaction Rate Coefficient function	$K^*_r(\theta_w)$	1/s
Solubility Coefficient[1]	S	
Decay Half-Life	$t_{1/2}$	s
Longitudinal Dispersivity in Air Phase	α_{La}	m
Transverse Dispersivity in Air Phase	α_{Ta}	m
Longitudinal Dispersivity in Water Phase	α_{Lw}	m
Transverse Dispersivity in Water Phase	α_{Tw}	m

[1]Henry's law constant expressed as the dimensionless ratio between the aqueous-phase concentration of a species and its gas-phase concentration

6.3 Boundary Conditions

The first type boundary condition in a solute and gas transfer analysis is specification of the primary variable; that is, concentration. Specification of the gradient in concentration normal to the boundary is a second type boundary condition and specification of the mass flux, or mass rate, at the boundary is the third type boundary condition.

The divergence and convective forms of the transport equation are physically equal but lead to different boundary condition formulations. In contrast to the divergence form (solute transfer), the convective form (gas transfer) inherently allows mass to leave the domain by advection with flowing water or air. In other words, the default boundary condition is zero dispersive mass flux. A mass flux (q) or mass rate (Q) boundary condition with a value of 0.0 must therefore be applied to achieve a total mass flux of zero. Incidentally, the same behaviour exists in a TEMP/W analysis involving heat advection with flowing water or air; that is, heat can leave or enter the domain with flowing fluid at the default second type boundary. There are two additional CTRAN/W boundary conditions for both solute and gas transfer analyses that require further consideration: (1) source concentration; and (2) free exit mass flux.

6.3.1 Source Concentration

The source concentration is a special form of the third type boundary in which the mass flux entering the domain is calculated as the fluid flux multiplied by the input source concentration.

$$J_s = Cq_n \qquad \text{Equation 125}$$

This boundary condition is useful because the concentration of the pore-fluid at the edge of the boundary is not necessarily equal to the source concentration at the onset of an analysis due to mass flux produced by concentration gradients. It is like a mass flux (q) or mass rate (Q) boundary in that the boundary condition controls the mass flux into the domain; however, in this case the user is specifying the concentration of the fluid external to the domain and allowing the software to calculate mass flux with the fluid flowing across the domain boundary.

6.3.2 Free Exit Mass Flux

The free exit boundary condition allows mass to exit by advection in accordance with the solute concentration arriving at the boundary:

$$J_s = Cq_n \qquad \text{Equation 126}$$

where the fluid flux, q_n, is calculated normal to the surface. The free exit mass flux boundary condition does not require any inputs because the concentration at the boundary is computed by the solver. The free exit boundary condition reverts to a zero total mass flux boundary condition if fluid is entering the domain, which causes a flushing effect given that the fluid is implicitly at zero concentration. As noted in 6.3, the gas transfer formulation inherently allows mass to leave the domain by advection, making the free exit boundary condition redundant.

6.4 Convergence

Appendix I.8 provides an overview on the convergence settings and under-relaxation controls to obtain a converged solution. The finite element solution of the advection-dispersion equations can produce numerical dispersion and oscillation that cannot be detected by the convergence criteria. These numerical problems must be detected by some other means, specifically the use of dimensionless numbers.

6.4.1 Dimensionless Numbers

The Péclet and Courant dimensionless numbers can be used to minimize the numerical dispersion and oscillation that is inherent in the finite element solution of the advection-dispersion equation. The Péclet number is defined as the ratio of the rate of advection to the rate of diffusion, and thus provides a measure of the degree to which advection dominates the contaminant transport process. The Courant number, on the other hand, reflects the portion of an element that is traversed by a solute in one time step. In one dimensional form, these numbers read as follows

$$\begin{aligned} \mathrm{Pe} &\equiv \mathrm{ReSc} \\ \square &= \frac{v\Delta x}{\eta/\rho}\frac{\eta/\rho}{D} \\ \square &= \frac{v\Delta x}{D} \end{aligned} \qquad \text{Equation 127}$$

$$\mathrm{C} = \frac{v\Delta t}{\Delta x}$$

where Re and Sc are the Reynolds and Schmidt dimensionless numbers, respectively; v is the fluid velocity; Δx is the nodal spacing; η is the dynamic viscosity of the fluid; ρ is the mass density of the fluid; D is the coefficient of hydrodynamic dispersion; Δt is the time increment. Ensuring that the Péclet number remains smaller than two (2) and the Courant number smaller than one (1) decreases oscillations, improves accuracy and decreases numerical dispersion when advection dominates dispersion. In other words, the spatial discretization of the flow regime should not be larger than twice the dispersion potential of the porous media and the distance traveled by advection during one time step.

7 References

Allen, R.G., Pereira, Luis S., Raes, D. and Smith, M. 1998. Crop evapotranspiration - Guidelines for computing crop water requirements - FAO Irrigation and drainage paper 56. Food and Agriculture Organization of the United Nations.

Andersland, O.B. and Ladanyi, B. 2004. Frozen Ground Engineering, 2nd Edition. John Wiley and Sons Inc., New Jersey.

Aubertin, M., Aachib, M. and Authier, K. 2000. Evaluation of diffusive gas flux through covers with a GCL. Geotextiles and Geomembranes, 18: 1-19.

Aubertin, M., Mbonimpa, M., Bussière, B. and Chapuis, R.P. 2003. A model to predict the water retention curve from basic geotechnical properties. Canadian Geotechnical Journal, 40(6): 1104-1122.

Barbour, S.L. and Fredlund, D.G. 1989. Mechanisms of osmotic flow and volume change in clay soils. Canadian Geotechnical Journal, 26: 551-552.

Barbour, S.L. and Krahn, J. 2004. Numerical modelling: Prediction or process? Geotechnical News, December: 44-52.

Bathe, K.J. 2006. Finite Element Procedures. Prentice Hall, Pearson Education Inc.

Ba-Te, B., Zhang, L. and Fredlund, D.G. 2005. A general air-phase permeability function for air flow through unsaturated soils. Geotechnical Special Publication no. 130 – 142, Geo-Frontiers 2005: 2961-2985.

Bear, J. 1988. Dynamics of Fluids in Porous Media. American Elsevier Publishing Company, Inc., New York.

Bear, J. 1979. Hydraulics of Groundwater. McGraw-Hill, New York.

Bowles, J.E. 1988. Foundation analysis and design. Fourth Edition. McGraw-Hill, Inc.

Brutsaert, W. 1975. The roughness length for water vapor, sensible heat and other scalars, Journal of Atmospheric Sciences. 32: 2028-2031.

Buck, A. L. 1981. New equations for computing vapor pressure and enhancement factor. Journal of Applied Meteorology, 20: 1527-1532.

Burland, J.B. 1987. Nash Lecture: The Teaching of Soil Mechanics – a Personal View. Proceedings of the 9th ECSMFE, Dublin, vol. 3, pp. 1427-1447.

Burland J.B. 1996. Closing Session Discussions. In: Proceedings of the First International Conference on Unsaturated Soils, Paris, 6-8 September 1995. Edited by E.E. Alonso and P. Delage. A.A. Balkema. vol. 3, pp. 1562-1564.

Carslaw, H.S. and Jaeger, J.C. 1986. Conduction of Heat in Solids, Oxford Science Publication, 2nd Edition.

Côté, J. and Konrad, J.-M. 2005. A numerical approach to evaluate the risk of differential surface icing on pavements with insulated surfaces. Cold Regions Science and Technology, 43: 187-206.

Desai, C.S. 1979. Elementary Finite Element Method. Prentice-Hall Inc., Englewood Cliffs, N.J.

de Vries, D.A. 1963. Thermal Properties of Soils. *In* The Physics of Plant Environment. Edited by W.R. van Wijk. Amsterdam, p. 382.

de Vries, D.A. 1975. Heat Transfer in Soils. *In* Heat and Mass Transfer in the Biosphere, 1. Transfer Process in Plant Environment. Washington, DC, pp. 5-28.

Dingman, S.L. 2008. Physical Hydrology, 2nd Edition. Waveland Press Inc., Long Grove, Illinois.

Domenico, P.A. and Schwartz, W. 1998. Physical and Chemical Hydrogeology. 2nd Edition. John Wiley & Sons Inc., New York.

Farouki, O.T. 1981. Thermal Properties of Soils. CRREL Monograph 81-1. U.S. Army Corps of Engineers, Cold Regions Research and Engineering Laboratory, Hanover, New Hampshire.

Food and Agriculture Organization of the United Nations, 1998. Crop Evapotranspiration: Guidelines for computing crop water requirements.

Fayer, M.J. 2000. UNSAT-H version 3.0: Unsaturated soil water and heat flow model, theory, user manual, and examples, Rep. 13249, Pacific Northwest National Laboratory, Richland, Washington.

Feddes, R.A., Hoff, H., Bruen, M., Dawson, T. de Rosnay, P., Dirmeyer, P., Jackson, R.B., Kabat, P., Kleidon, A., Lilly, A. and Pitman, A.J. 2001. Modeling root water uptake in hydrological and climate models. Bulletin of the Americal Meteorological Society, 82(12): 2797 – 2809.

Flerchinger, G.N., Kustas, W.P. and Weltz, M.A. 1998. Simulating surface energy fluxes and radiometric surface temperatures for two arid vegetation communities using the SHAW model. Journal of Applied Meteorology, 37: 449-60.

Flerchinger, G.N. 2000. The Simultaneous Heat and Water Model: Technical Documentation.

Flerchinger, G.N., Seyfried, M.S. and Hardegree, S.P. 2006. Using soil freezing characteristics to model multi-season soil water dynamics. Vadose Zone Journal, 5: 1143-1153.

Fredlund, D.G. and Rahardjo, H. 1993. Soil Mechanics for Unsaturated Soils. John Wiley & Sons, Inc. NJ.

Fredlund, D.G., Rahardjo, H. and Fredlund, M.D. 2012. Unsaturated Soil Mechanics in Engineering Practice. John Wiley & Sons, Inc. NJ.

Fredlund, D.G. and Xing, A. 1994. Equations for the soil-water characteristic curve. Canadian Geotechnical Journal, 31, 521-532.

Fredlund, D.G., Xing, A. and Huang, S. 1994. Predicting the permeability function for unsaturated soils using the soil-water characteristic curve. Canadian Geotechnical Journal, 31(4), 533-546.

Freeze, R.A. and Cherry, J.A. 1979. Ground Water. Englewood Cliffs, NJ: Prentice Hall.

Frind, E.O. 1988. Solution of the advection-dispersion equation with free exit boundary. Numerical Methods for Partial Differential Equations, 4: 301-313.

Hansson, K., Simunek, J., Mizoguchi , M., Lundin, L.-C. and van Genuchten, M.Th. 2004. Water flow and heat transport in frozen soil: Numerical solution and freeze-thaw applications. Vadose Zone Journal, 3: 693-704.

Harlan, R.L. and Nixon, J.F. 1978. Ground Thermal Regime. Geotechnical Engineering for Cold Regions, Edited by O.B. Andersland and D.M. Anderson. McGraw-Hill Inc.

Haynes, F.D. and Zarling, J.P. 1988. Thermosyphons and foundation design in cold regions. Cold Regions Science and Technology, 15: 251-259.

Hughes, T.J.R. 2000. The Finite Element Method: Linear Static and Dynamic Finite Element Analysis. Dover Publications. Mineola, New York.

Idso, S.B. 1981. A set of equations for full spectrum and 8- to 14-µm and 10.5- to 12.5-µm thermal radiation from cloudless skies. Water Resources Research, 17: 295-304.

Incropera, F.P., DeWitt, D.P., Bergman, T. L. and Adrienne, S. L. 2007. Fundamentals of Heat and Mass Transfer, 6th Edition. John Wiley & Sons Inc. New Jersey, USA.

Johansen, O. 1975. Thermal Conductivity of Soils. Ph.D. thesis. Trondheim, Norway. (CRREL Draft Translation 637, 1977), ADA044002.

Johnston, G.H., Ladanyi, B., Morgenstern, N.R. and Penner, E. 1981. Engineering Characteristics of Frozen and Thawing Soils. Permafrost Engineering Design and Construction. Edited by Johnston, G.H. John Wiley & Sons.

Joshi, B., Barbour, S.L., Krause A.E. and Wilson G.W. 1993. A finite element model for the coupled flow of heat and moisture in soils under atmospheric forcing. Finite Elements in Analysis and Design, 15: 57-68.

Jury, W.A. and Horton, R. 2004. Soil Physics, 6th Edition. John Wiley & Sons Inc. New Jersey, USA.

Kimball, B.A., Jackson, R.D., Reginato, R.J., Nakayama, F.S. and Idso, S.B. 1976. Comparison of field measured and calculated soil heat fluxes. Soil Science Society of America Journal, 40: 18-25.

Kelleners, T.J., Chandler, D.G., McNamara, J.P., Gribb, M.M. and Seyfried, M. 2009. Modeling the water and energy balance of vegetated areas with snow accumulation. Vadose Zone Journal, 8(4): 1013-1030.

Kézdi, Á. 1974. Handbook of soil mechanics. Elsevier Scientific, Amsterdam.

Koivusalo, H., Heikinheimo, M. and Karvonen, T. 2001. Test of a simple two-layer parameterization to simulate the energy balance and temperature of a snow pack. Theoretical and Applied Climatology, 70: 65-79.

Lai, S.H., Tiedje, J.M. and Erickson, A.E. 1976. In situ measurement of gas diffusion coefficient in soils. Soil Science Society of America Journal, 40: 3-6.

Lebeau, M. and Konrad, J.-M. 2007. The effects and significance of natural convection in rockfill dams under cold climate conditions. Proceedings of the 60th Canadian Geotechnical Conference & 8th Joint CGS/IAH-CNC Groundwater Conference. Ottawa, Ontario, Canada. October 21 – 24, 2007.

Lewis, R.W., Nithiarasu, P. and Seetharamu, K.N. 2004. Fundamentals of the Finite Element Method for Heat and Fluid Flow. John Wiley & Sons, Inc. NJ.

Liu, S., Graham, W.D. and Jacobs, J.M. 2005. Daily potential evapotranspiration and diurnal climate forcings: influence on the numerical modelling of soil water. Journal of Hydrology, 309: 39-52.

Monteith, J.L. 1981. Evaporation and surface temperature. Quarterly Journal of the Royal Meteorological Society, 107: 1-27.

Nassar, I.N. and Horton, R. 1989. Water transport in unsaturated nonisothermal salty soil: II. Theoretical development. Soil Science Society of America Journal, 53: 1330-1337.

Nassar, I.N. and Horton, R. 1992. Simultaneous transfer of heat, water, and solute in porous media: I. Theoretical development. Soil Science Society of America Journal, 56: 1350-1356.

Newman, G.P. 1995. Heat and mass transfer in unsaturated soils during freezing. M.Sc. Thesis, University of Saskatchewan, Saskatoon, Canada.

Penman, H.L. 1948. Natural evaporation from open water, bare soil, and grass. Proceedings of the Royal Society of London, Series A: Mathematical and Physical Sciences, 193: 120-145.

Philip, J.R. and de Vries, D.A. 1957. Moisture Movement in Porous Materials under Temperature Gradients. Transactions American Geophysical Union, 38(2): 222-232.

Ritchie, J.T. 1972. Model for predicting evaporation from a row crop with incomplete cover. Water Resources Research, 8(5): 1204-1213.

Ritter, M.E. The Physical Environment: an Introduction to Physical Geography. 2006. Date Visited: December 19, 2008. http://www.uwsp.edu/geo/faculty/ritter/geog101/textbook/title_page.html

Saito, H., Simunek, J. and Mohanty, P. 2006. Numerical analysis of coupled water, vapor, and heat transport in the vadose zone. Vadose Zone Journal, 5: 784-800.

Saito, H. and Simunek, J. 2009. Effects of meteorological models on the solution of the surface energy balance and soil temperature variations in bare soils. Journal of Hydrology, 373: 545-561.

Schofield, R.K. 1935. The PF of the water in soil. Transactions of the 3rd. International Congress of Soil Science, 2: 37-48.

Sellers, W.D. 1965. Physical Climatology. University of Chicago Press. Chicago, Illinois.

Šimůnek, J., Šejna, M., Saito, H., Sakai, M. and van Genuchten, M.T. 2012. The HYDRUS-1D Software Pack for Simulating the One-Dimensional Movement of Water, Heat, and Multiple Solutes in Variably-Saturated Media (Version 4.15).

Smith, I.M. and Griffiths, D.V. 2014. Programming the Finite Element Method. 5th Edition. John Wiley & Sons Ltd.

Spaans, E.J.A. and Baker, J.M. 1996. The soil freezing characteristic: its measurement and similarity to the soil moisture characteristic. Soil Science Society of America Journal, 60: 13 -19.

Thornthwaite, C.W. 1948. An approach toward a rational classification of climate. Geographical Review, 38: 55-94.

van Bavel, C.M. and Hillel, D.I. 1976. Calculating potential and actual evaporation from a bare soil surface by simulation of concurrent flow of water and heat. Agricultural Meteorology, 17: 453-476.

van Genuchten, M.Th. 1980. A closed-form equation for predicting the hydraulic conductivity of unsaturated soils. Soil Science Society of America Journal 44(5): 892-898.

Williams, P.J. and Smith, M.W. 1989. The frozen earth—Fundamentals of geocryology. Cambridge University Press, Oxford.

Wilson, G.W. 1990. Soil Evaporative Fluxes for Geotechnical Engineering Problems. Ph.D. Thesis, University of Saskatchewan, Saskatoon, Canada.

Wilson, G.W., Fredlund, D.G. and Barbour, S.L. 1997. The effect of soil suction on evaporative fluxes from soil surfaces. Canadian Geotechnical Journal, 34: 145-155.

Zienkiewicz, O. C. and Taylor, R.L. 1989. The Finite Element Method: Basic Formulation and Linear Problems. 4th Edition. McGraw-Hill Book Company. London, UK.

Appendix I Formulation Fundamentals

There have been many thorough textbooks written on the subject of the finite element method (e.g. Bathe, 2006; Zienkiewicz and Taylor, 1989). The method is mathematically elegant and generalized; however, the details of the derivations and implementation strategies can be overwhelming. As such, the objective of this appendix is to provide a basic overview of the method with the goal being to provide a framework for discussing other topics such as discretization, the need for a constitutive model, and boundary conditions.

An analytical or closed-form solution of a physical problem always involves a few common steps. First, a set of mathematical equations must be derived to describe the physical process under consideration; commonly this takes the form of a partial differential equation (PDE) expressed in terms of some dependent variable. Next, the temporal and spatial limits of the problem (the domain over which the solution is sought) is defined and the appropriate boundary conditions which constrain the solution are defined. All parameters within the PDE must then be defined, including material properties used to characterize a particular material behavior. The solution of the PDE over the domain, given the specified material properties and subject to the selected boundary conditions, is the value of the dependent variable as a function of position and time (in the case of a transient problem).

A similar solution pattern is applied in the case of the FEM. A conceptual model of a physical system is developed, the relevant physics (PDE) are selected, and the domain for the solution is defined. Just as in the analytical solution, the material properties across the domain must be specified and boundary conditions must be applied to constrain the solution. The FEM is selected as a solution method, rather than an analytical solution, likely due to complexities in geometry or material behavior. In order to overcome these complexities, the FEM, essentially, 'solves' the governing equation over smaller 'finite elements' which have well defined geometry and have a pre-selected shape to the distribution of the dependent variable across the element. The PDE across an individual element is then described in terms of the values of the dependent variable at the element nodes (fixed positions within the domain). Solving for the common set of nodal values for all elements at the same time then results in the solution of the dependent variable across the domain (i.e. in space and time).

As a consequence, the finite element method involves the following general steps:

1. Discretization of the domain into finite elements;
2. Selection of a function to describe how the primary variable varies within an element;
3. Definition of a constitutive relationship;
4. Derivation of element equations;
5. Assembly of the global equations and modification for boundary conditions; and,
6. Solution of the global equations.

The solution of the global equations, which is a solution to a partial differential equation, provides a spatial and temporal description of the primary variable (e.g. temperature or displacement) within the domain.

I.1 Governing Equation

The governing partial differential equations for heat and mass transfer formulations are derived from the requirement for energy or mass conservation. The following sections provide generalized descriptions of the conservation requirements.

I.1.1 Conservation of Mass Requirement

The governing equations for the water (Section 3), air (Section 5), solute (Section 6), and gas (Section 6) transfer formulations are derived from the requirement for mass conservation. The law of mass conservation states that the total mass of a system is conserved and that the mass in a system can only change if mass crosses its boundaries. The principle of mass conservation states that the increase in the mass stored in a control volume must equal the mass that enters the control volume, minus the mass that leaves the control volume, plus the mass that is added (source or sink) to the control volume (Incropera et al., 2007).

The principle of mass conservation must also be satisfied at every instant of time, which means that there must be a balance between all mass rates (i.e. mass per time). This can be stated as follows: the rate of increase in the mass stored in a control volume must equal the mass rate entering the control volume, minus the mass rate leaving the control volume, plus the mass rate at which mass is added to the control volume.

The generic mass conservation statement in equation form is provided in Section 3.1 (Equation 1); however, this statement can be specialized by appending 'of water', 'of air', 'of dissolved solute', or of 'gas' for the corresponding transfer formulation. The inflow and outflow terms in Equation 1 (m_{in} and m_{out}) can be separated into the mass transfer rates perpendicular to the control volume surfaces in the x, y, and z directions ($\dot{m}_x$, $\dot{m}_y$, and $\dot{m}_z$). The mass rates at the opposite surfaces can then be expressed as a Taylor series expansion. Neglecting higher order terms and considering only one-dimensional flow in the y-coordinate direction, the mass rate at the opposite surface is given by:

$$\dot{m}_{y+dy} = \dot{m}_y + \frac{\partial \dot{m}_y}{\partial y} dy \qquad \text{Equation 128}$$

Expressing the principle of mass conservation (Equation 1) with the foregoing rate equations and assuming that no mass is added to (or removed from) the control mass, gives:

$$\dot{M}_{st} = \dot{m}_y - \dot{m}_{y+dy} \qquad \text{Equation 129}$$

Substitution of Equation 128 into Equation 129 gives:

$$\dot{M}_{st} = -\frac{\partial \dot{m}_y}{\partial y} dy \qquad \text{Equation 130}$$

Equation 130 is generalized for the transient condition, which implies a temporal change in the stored mass. Changes in stored mass are the result of a time-dependency of the primary variable. A well-known example of this in geotechnical engineering would be consolidation – the time-dependent dissipation of excess pore-water pressure and concomitant time-dependent compression of a soil profile. Analogous processes include redistribution of solute or gas within a porous media and air/water pressure changes due to barometric pressure changes. A steady-state condition develops when the mass or energy stored within a system is constant. This can only occur if the primary variable at each point in space is independent of time. The steady-state rate-based mass conservation statement can be written as:

$$0 = -\frac{\partial \dot{m}_y}{\partial y} dy \qquad \text{Equation 131}$$

I.1.2 Conservation of Energy Requirement

A similar conservation equation and approach can be applied to energy transport. There are various forms of energy transport (e.g. thermal, electrical, chemical); however, TEMP/W considers only thermal energy, comprised of sensible and latent components. The energy in a system changes according to the first law of thermodynamics, which states that the increase in the amount of thermal energy stored in a control volume must equal the amount of thermal energy that enters the control volume, minus the amount of thermal energy that leaves the control volume, plus the amount of thermal energy that is generated within the control volume (Incropera et al., 2007).

Energy is quantified in the SI system in terms of joules. The first law must also be satisfied at every instant of time, which means that there must be a balance between all energy rates, as measured in joules per second (Watts, W). In words, this is expressed as: The rate of increase in the amount of thermal energy stored in a control volume must equal the rate at which thermal energy enters the control volume, minus the rate at which thermal energy leaves the control volume, plus the rate at which thermal energy is generated within the control volume (Incropera et al., 2007).

The equation associated with the rate-based energy conservation statement is provided in Section 4.1 (Equation 50). The inflow and outflow terms in Equation 50 ($\dot{E}_{in}$ and $\dot{E}_{out}$) represent heat transfer processes across the control surfaces. These energy rates are perpendicular to each of the surfaces in the x, y, and z directions ($\dot{Q}_x$, $\dot{Q}_y$, and $\dot{Q}_z$). The conduction heat rates at the opposite surfaces can then be expressed as a Taylor series expansion. Neglecting higher order terms and considering only one-dimensional flow in the y-coordinate direction, the heat rate at the opposite surface is given by:

$$\dot{Q}_{y+dy} = \dot{Q}_y + \frac{\partial \dot{Q}_y}{\partial y} dy \qquad \text{Equation 132}$$

The rate at which thermal energy enters the control volume by energy advection – also termed forced convection – is calculated as $\dot{m}_y u_{t(y)}$, where u_t is the thermal energy per unit mass and $\dot{m}_y$ is the mass

flow rate. The rate at which thermal energy exits the control volume at the opposite surfaces can be expressed as a Taylor series expansion:

$$\dot{m}_{y+dy}u_{t(y+dy)} = \dot{m}_y u_{t(y)} + \frac{\partial\left(\dot{m}_y u_{t(y)}\right)}{\partial y}dy \qquad \text{Equation 133}$$

where the higher order terms are neglected.

Expressing the conservation of energy (Equation 50) with the foregoing rate equations, assuming no energy generation within the control volume, gives:

$$\dot{E}_{st} = \dot{Q}_y + \dot{m}_y u_{t(y)} - \dot{Q}_{y+dy} - \dot{m}_{y+dy}u_{t(y+dy)} \qquad \text{Equation 134}$$

Substitution of Equation 132 and Equation 133 into Equation 134 gives:

$$\dot{E}_{st} = -\frac{\partial \dot{Q}_y}{\partial y}dy - \frac{\partial\left(\dot{m}_y u_{t(y)}\right)}{\partial y}dy \qquad \text{Equation 135}$$

A transient response of a physical system is indicated by temporal changes in energy. Therefore, temperature is time-dependent. The propagation of a freezing front is an example of a well-known transient phenomenon. A steady-state condition develops when the energy within a system is constant. This can only occur if the temperature at each point in space is independent of time. The steady-state rate based energy conservation statement can be written as:

$$\dot{E}_{st} = 0 = -\frac{\partial \dot{Q}_y}{\partial y}dy - \frac{\partial\left(\dot{m}_y u_{t(y)}\right)}{\partial y}dy \qquad \text{Equation 136}$$

I.2 Domain Discretization

The essence of the finite element method is embodied by discretization. Discretization is the process of subdividing a complex system into a number of finite elements. Figure 9 shows an 8-node quadrilateral and 6-node triangular element. Subdivision of the system into finite elements makes it possible to solve the governing equation by writing equations for each individual finite element. The term discretization implies approximation because the finite element method solves for the independent variable at discrete points (the element nodes) within the domain. This produces a piece-wise approximation of a variable, which in reality is continuously distributed (e.g., concentration or air pressure).

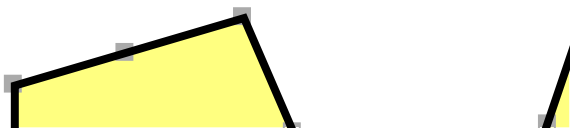

Figure 9. Examples of finite elements.

I.3 Primary Variable Approximation

The primary variable is calculated only at the element nodes. Thus, a shape or interpolation function is required to generate a continuously distributed approximation of the primary variable. The interpolation function describes the spatial variation of the primary variable within the element and is used to estimate its value between the known data points (i.e., the nodes). Interpolation of a primary variable is given by:

$$u = \sum_{i=1}^{q} h_i u_i \qquad \text{Equation 137}$$

where u is the is the primary value anywhere within the element, u_i is the value at nodal points, and h_i is the interpolating function for that particular node. A function of this form is written for all primary variables, if there are more than 1 (e.g., displacement in the direction of the three primary coordinates). The mathematical descriptions of the interpolating functions are irrelevant to this discussion. The key concept is that the primary variable anywhere within the element is described based on nodal values.

I.4 Element Equations

The solution of a partial differential equation by the finite element method ultimately produces an equation for each element. Bathe (2006) provides an insightful and generalized derivation of the finite element equation for a steady-state problem, which can be written using matrix notation as:

$$\boldsymbol{K}^{(m)}\boldsymbol{U}^{(m)} = \boldsymbol{R}^{(m)} \qquad \text{Equation 138}$$

where $\boldsymbol{K}^{(m)}$ is the element characteristic matrix, $\boldsymbol{U}^{(m)}$ is the matrix of nodal unknowns, $\boldsymbol{R}^{(m)}$ is the nodal load vector for the element, which is sometimes called the forcing vector or the resultant vector. The matrix notation represents a set of simultaneous algebraic equations that can be solved using a number of techniques. The element characteristic matrix comprises a number of terms, including the constitutive matrix, $\boldsymbol{C}^{(m)}$, that is populated with the material properties. The finite element equation for a transient heat or mass transfer problem takes the form:

$$\boldsymbol{K}^{(m)}\boldsymbol{U}^{(m)} - \boldsymbol{M}^{(m)}\dot{\boldsymbol{U}}^{(m)} = \boldsymbol{R}^{(m)} \qquad \text{Equation 139}$$

The over dot indicates a time derivative of the primary variable and $\boldsymbol{M}^{(m)}$ is the element mass matrix. The mass matrix embodies the material property related to storage. The time derivative of the primary variable is the difference between the value at the current time step and the previous time step, divided by the time increment. As a result of the time derivative, a transient analysis requires: a) time-step definition; and, b) initial conditions.

Although not revealed by this basic discourse, and regardless of the complexity of the final form of the equation, the element equation is in fact a perfect reflection of the conservation statement on which it was derived. In other words, it is possible to inspect the mathematical operations and recover the

conservation statement. Desai (1979) provides a more elementary derivation that lends clarity to the idea that the element equation is a perfect reflection of the conservation statement.

I.5 Global Equations

One of the most elegant aspects of the finite element method lies in Step 5: assembly of the global finite element equation. The element equations (Equation 139) are generated recursively for every element in the domain and then added to the global finite element equation:

$$\boldsymbol{KU} = \boldsymbol{R} \qquad \text{Equation 140}$$

where $\boldsymbol{K}$ is the global characteristic matrix, $\boldsymbol{U}$ is the global assemblage of nodal unknowns, and $\boldsymbol{R}$ is the global load vector.

The assembly process is based on the law of compatibility or continuity. The assembly process can also be considered the final step required to obey the governing partial differential equation, which applies to the entire domain (i.e., not just one element). The global finite element equation satisfies the governing partial differential equation because it is the result of assembling the individual equations for a single element that were formulated to satisfy the governing PDE. The assembly procedure is analogous to the method of sections used to analyze the static equilibrium of a truss. Equilibrium of the entire system is ensured by satisfying static equilibrium for each member of the structure.

Assembly of the finite element equations requires material property and element geometry definitions. Conveniently, the discretization process produces a collection of elements and nodes with defined geometry, namely the Cartesian coordinates of all the nodes.

It is important to note that the global finite element equation shown above is essentially a set of n equations where n is the number of nodes. The $\boldsymbol{U}$ vector represents the n primary variables and the R vector represents the nodal fluxes. Consequently, the only way a solution can be sought for this set of linear equations is to have no more than n unknowns; consequently, a value of the primary variable or the nodal flux must be known (specified) at every node. The final step of the finite element procedure (Step 6) is specification of the physical constraints to the solution at all nodes (i.e., boundary conditions) to solve the global equations to obtain a spatial description of the primary variable.

Consider, for example, a simple domain in which the primary unknown is specified uniquely at two nodes on the left side and two nodes on the right side of the domain (Figure 10). Solution of Equation 139 subject to these boundary conditions produces the primary variable at all nodes at which the primary variable is unknown. Since the left and right-side nodes had a specified value of the dependent variable, the flow rate at these nodes is unknown; while, in the interior nodes the value of the dependent variable is unknown; however, to satisfy the conservation of mass, the net flow at these nodes is zero. Subsequent assembly of Equation 140 produces the flow rates at all nodes. The flow rates at the boundary nodes are non-zero because there is no adjacent element that apportions a flow rate with equal magnitude and opposite sign to cause cancellation.

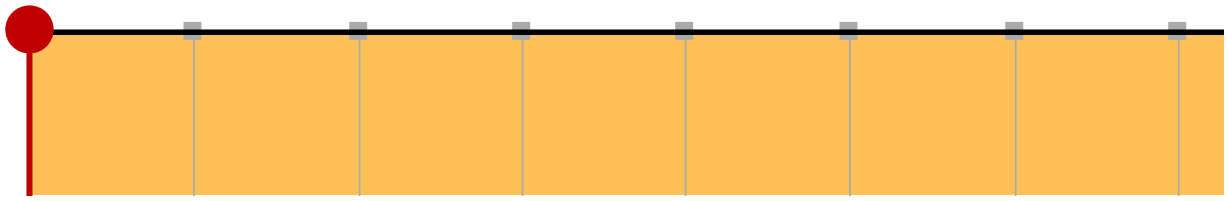

Figure 10. A simple finite element domain with boundary conditions on the left and right sides.

In summary, the finite element method is a procedure for solving a partial differential equation, which is a mathematical expression that governs the response of a physical system. Naturally, analysts seek to describe and analyze the behavior of these systems. The key aspects of the finite element method are:

1. The partial differential equation describing the behavior of a physical system can be solved, using the finite element method, by discretizing the domain into finite elements.
2. The process of discretization implies approximation; that is, the solution to the finite element equation provides the approximate spatial distribution of the primary variable at the nodes.
3. The derivation of the finite element equations is based on a single element. The final equation embodies the material properties and element geometry.
4. Using the principle of compatibility, these element equations are written recursively for every element in the domain and assembled into the global finite element equation.
5. The global finite element equation is solved subject to boundary conditions.

I.6 Constitutive Behaviour

A constitutive model links a secondary quantity (e.g., flux) to the primary variable (e.g., temperature) or changes in the primary variable to changes in the stored mass or energy. As a result, constitutive models must represent two material behaviours: flow and storage. The storage component is only required for a transient analysis.

Problems involving mass or energy transfer require a constitutive model that links a volume or energy flux to an energy gradient. By way of comparison, stress-strain problems require a constitutive law that links incremental stress changes to incremental strain quantities. Fourier's Law, Fick's law, and Darcy's law are examples of flow laws that govern heat, solute, and water flow, respectively. The flow laws generally contain a property of the material through which flow is occurring – a coefficient – that ensures proportionality between the energy gradients and the resulting mass or energy flux. Hydraulic and thermal conductivity and the coefficient of diffusion are examples of such coefficients. These coefficients may be constants or functions of other parameters and may therefore be directly or indirectly functions of the primary variable. For instance, thermal conductivity may vary with the proportions of ice and liquid water within the pore-space and is consequently a function of the unfrozen water content, or indirectly a function of temperature.

Transient problems require a constitutive model that links time-dependent changes in the energy or mass stored in the system to the primary variable. In the case of heat transfer, there must be an increase in the amount of thermal energy stored in an element if the temperature of the element increases. Similarly, the volumetric water content function links the change in the mass of water to changes in pore-water pressure. There are several different material models in each product to accommodate different ways of parameterizing the flow and storage properties.

I.6.1 Functional Relationships

Many of the constitutive models in GeoStudio require a functional relationship between a material property and some other parameter. For example, water hydraulic conductivity can be defined as a function of matric suction and thermal conductivity can be made to vary with either temperature or volumetric water content. Functional relationships are defined by a data set that relates the property to a parameter. The software then represents the data by a computed functional relationship, $f(x)$ (e.g., polynomial spline, linear interpolation, step function), which is used by the solver.

The data points defining the functional relationship can be from a measured dataset or generated by published empirical or semi-empirical methods. In some cases, the software provides an estimation routine. The estimation routines are documented in the product-specific sections.

I.6.2 Add-ins

User-defined functional relationships, such as those mentioned in Section I.6.1, can be generated by an Add-In. An Add-In is compiled computer code called by the solver. A material function add-in returns a specific property (e.g., thermal conductivity) at every gauss point within every element to which the material model is assigned to the solver. The add-in can comprise a functional relationship that is multi-variable, of any mathematical form, and dependent on another variable from the analysis being solved or from another analysis.

I.7 Boundary Conditions

GeoStudio can be used to analyze a variety of field problems to define the state variable spatially within the domain. The state variable may be a vector or scalar, where a vector has both magnitude and direction (e.g., forces/stresses in SIGMA/W), while a scalar has only magnitude (e.g., total head in SEEP/W).

In the analysis of field problems, the values of the state variables are generally given on the boundaries. An example would be the total head along the ground surface of a reservoir impoundment or the vertical stress beneath a rigid foundation. Accordingly, these problems are called boundary value problems, where the solution within the domain depends on the conditions along the boundary of the domain (Bathe, 2006). A change in only one boundary value affects the entire solution.

I.7.1 Types

There are fundamentally three types of boundary conditions used in a finite element analysis:

1. First-type;
2. Second-type; and,
3. Third-type.

Consider the global finite element equation (Equation 140) that comprises the global assemblage of nodal unknowns (U) and the global load vector (R). A first-type boundary condition specifies the primary unknown at a node and is used to populate the U vector. A second-type boundary condition is the spatial derivative of the primary variable normal to the boundary. In the case of scalar problems, this would be equivalent to applying a flux. Second-type boundary conditions are applied over an area and apportioned to nodes via numerical integration. These boundary values are used to populate the R vector. Finally, a third-type boundary condition specifies a nodal value directly in the global load vector. Table 21 summarizes the fundamental boundary conditions in each GeoStudio product, while the product-specific sections detail boundary conditions unique to each product.

Table 21. Boundary condition types for each GeoStudio application.

Application	First-type	Second-type	Third-type
SEEP/W	Pore-water Total Head	Water Flux	Water Rate
TEMP/W	Temperature	Heat Flux	Heat Rate
AIR/W	Pore-air Total Head	Air Flux	Air Rate
CTRAN/W	Concentration	Mass Flux	Mass Rate
SIGMA/W	Displacement	Stress	Force
QUAKE/W	Displacement	Stress	Force

Boundary values can be defined as constants or functions. A constant boundary condition implies that the state of the boundary remains the same throughout the analysis. Functions are generally used in transient analyses to define the boundary-type as a function of time, but functions also have an important role in a SIGMA/W load-deformation or coupled analysis. Finally, it should be noted that even the most involved boundary conditions, such as the surface energy balance boundary in TEMP/W or the unit gradient boundary in SEEP/W, ultimately reduces to one of the three fundamental types. The surface energy balance boundary condition, for example, is a heat flux (second-type) boundary.

I.7.2 Add-ins

User-defined boundary conditions can be generated by an Add-In. A boundary condition add-in returns a specific value to the solver for every node (First or Third Type) or gauss point (Second Type) within every element to which the boundary condition is applied. The add-in can comprise a functional

relationship that is multi-variable, of any mathematical form, and may be dependent on another variable from the analysis being solved or from a different analysis.

I.8 Impervious Barriers

An impervious barrier prevents heat and/or mass transfer across a face in the domain, which is a point and a line in a 1D and 2D geometry, respectively. The barrier can be designated as impervious to water, heat, air, solute, and/or gas transfer depending on the physics being solved on the domain. An impervious barrier can be used, for example, to simulate a cut-off wall under a dam, an insulated (i.e. adiabatic) surface around a foundation, or an impervious diaphragm wall installed in an excavation.

I.9 Convergence

The global assemblage of finite element matrices contains material properties that could be a function of the solution. A commonly used numerical procedure for coping with material non-linearity involves repeatedly solving the finite element equations and updating the material properties based on the solution at the previous iteration. This repeated substitution continues until the maximum number of iterations is reached or a converged solution is obtained. Convergence occurs when successive solutions are equal within a specified tolerance. The GeoStudio products determine convergence based on two parameters: significant figures and maximum difference.

I.9.1 Significant Figures

The desired significant figure for comparison of the primary variable is specified in GeoStudio. The significant figures represent the digits that carry meaning as to the precision of the number. Leading and trailing zeros simply provide a reference as to the scale of the number. Consider the number 5123.789. This number could be written to a precision of two, three, or four significant figures as 5.1×10^3, 5.12×10^3, and 5.124×10^3, respectively. For example, specifying two significant digits means that when the primary variable at a node from two successive iterations is the same to a precision of two significant figures, the node is deemed to be converged.

I.9.2 Maximum Difference

Computer computations inherently produce numerical noise; that is, digits that have no significance. It is necessary to filter out the insignificant digits when comparing floating point numbers. GeoStudio filters out the insignificance using a user-specified maximum tolerable difference. If the difference between two successive primary variables at a node is less than this maximum tolerable difference, the two values are deemed to be numerically equivalent and the solution reaches convergence without giving consideration to the significant figure criteria. For example, a node would be designated as converged if the maximum difference was specified as 0.001 and the difference in the primary variable(s) between successive iterations was less than this value.

Consider two numbers such as 1.23×10^{-6} and 1.23×10^{-7}. These two numbers would not meet the significant figures criteria for convergence; however, the difference (1.11×10^{-6}) is small and may have no physical meaning in the context of the analysis. The two numbers are consequently deemed to be equivalent within the tolerance of the maximum difference.

I.9.3 Under-Relaxation

Successive iterative solutions can diverge and/or oscillate if the material properties are highly non-linear and dependent on the primary variable. Under-relaxation procedures attempt to mitigate large variations in the material properties on successive iterations. For example, the hydraulic conductivity of water in unsaturated soil can vary by many orders of magnitude over a small pore-water pressure range. The inclusion of latent heat effects in an energy transfer analysis is another example of extreme material non-linearity. Divergence of the solution after two successive iterations can therefore be mitigated by limiting – that is, under-relaxing – the variation of the material properties used to calculate the finite element matrices. This in turn exerts a control on the difference between successive solutions and produces a less chaotic progression towards a converged solution. The under-relaxation parameters are specified in the Convergence settings of the analysis definition and include:

1. Initial Rate (e.g., 1);
2. Minimum Rate (e.g., 0.1);
3. Rate Reduction Factor (e.g., 0.65); and,
4. Reduction Frequency (e.g., 10 iterations).

The Initial Rate essentially controls the allowable variation in material properties between successive iterations. A value of 1 corresponds to repeated substitution with no under-relaxation. The under-relaxation rate is reduced by multiplication of the Rate Reduction Factor once the Reduction Frequency is exceeded. For example, the under-relaxation rate would be 0.65 after the 10^{th} iteration, 0.65^2 after the 20^{th} iteration and so on until the under-relaxation rate is less than or equal to the minimum rate.

The default parameters may not be ideal for some numerically challenging problems. For example, it may be advantageous to immediately commence under-relaxation for a problem with highly non-linear material properties by specifying an Initial Rate less than 1 (e.g., 0.65). The Minimum Rate might also have to be reduced (e.g., 0.01) if the solution oscillates slightly around the final answer. Other variations on this strategy are possible, such as retaining the Initial Rate of 1 but reducing the Reduction Frequency (e.g. 5 iterations) and Minimum Rate (e.g., 0.01). Ultimately, some form of numerical experimentation is required and convergence must be judged by using the previously mentioned techniques.

I.9.4 Verifying Convergence

The general techniques for verifying convergence include:

1. Examining the number of nodes that met the convergence criteria (Sections I.9.2 and I.9.3) on two successive iterations;

2. Comparing iteration counts on each time step or reviewing to the maximum allowable value; and,
3. Examining the number of non-converged nodes with iteration.

These techniques are covered in material available on the GeoStudio website. Some products have additional techniques for verifying convergence.

Appendix II Numerical Modelling Best Practice

Burland (1987), in his seminal Nash Lecture, presented the idea that modelling is an integral part of geotechnical engineering practice (Figure 11). Geotechnical engineering involves defining the geological and hydrogeological system, understanding the constitutive behaviour of the material, and modelling. All three components are interlinked by experience. In the context of this discussion, the most prominent feature of this conceptualization is the fact that modelling is an integral part of the engineering process.

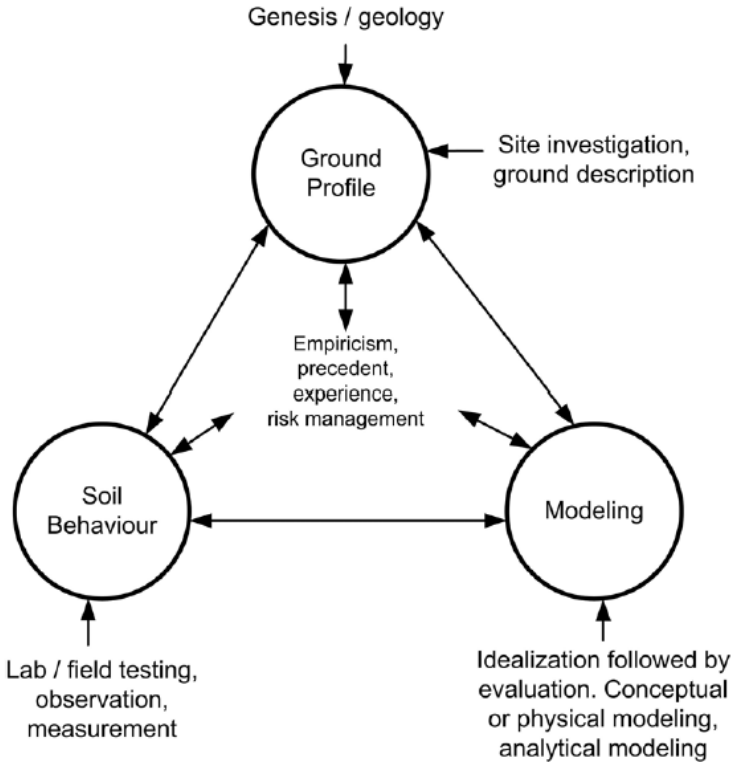

Figure 11. Burland Triangle (Ground Engineering, 1996).

Barbour and Krahn (2004) built upon the ideas of Burland (1996) and defined modelling as "the process by which we extract from a complex physical reality an appropriate mathematical reality on which we can base a design. The role of the numerical model is simply to assist us in developing the appropriate mathematical abstraction." Stated another way, a mathematical model is a simplified representation of a complex reality based on our understanding of the physical system.

This definition of modelling endorses the idea that modelling is about process, not prediction. The greatest strength of modelling is to develop the appropriate mathematical abstraction of a complex physical system. In turn, engineers are able to develop a sound understanding of the physical system and exercise better engineering judgment. The maximum benefit can only be achieved if modelling is incorporated into the entire problem solving process (Figure 11).

A finite element analysis is just one type of numerical model that is less restrictive and complimentary to other types of numerical models, such as analytical and graphical solutions. The primary reason for invoking a finite element analysis is to cope with various complexities, including: a) intricate geological and hydrogeological settings; b) nontrivial physical processes; c) multiple and competing design alternatives and economic implications; and, d) a decision making process that can be made difficult by the need to communicate ideas to regulators and the general public.

Barbour and Krahn (2004) elaborate on some of the intricacies of each of these complexities. It is perhaps worth highlighting that engineering problems involving the earth are particularly complicated because natural systems exhibit extreme spatial variability, complex and sometimes unquantifiable material behavior, incongruent temporal and spatial scales, and in many cases, physical processes that are not fully understood. Barbour and Krahn (2004) illustrate this realization with a poignant case history involving a comparison of various numerical simulations to measured deflections of a structurally supported retaining wall for a deep excavation. None of the predictions of the lateral deflections were accurate, or true to the measurements.

The reasons for the inaccuracies were related in part to the aforementioned complexities and conceptualization errors, and in part to numerical problems. One can conclude that, in general, predicting the exact response of a physical system is not feasible because it is impossible to reproduce all of the detail present in the physical problem in even the most refined mathematical model. Prediction should therefore not be the primary objective of numerical modelling. The encouraging aspect of the case history was that the overall patterns of the physical behaviour were adequately simulated. As such, the numerical solutions provided an appropriate basis for design.

This short discourse brings us back to the key advantage of numerical modelling: the process of numerical modelling enhances engineering judgement and provides a basis for understanding complicated physical processes. The process of modelling is iterative and comprises at least four essential components:

1. Define the modelling objective and develop a conceptual model of the problem;
2. Determine the appropriate theoretical models (i.e., physics) that describe the key physical processes;
3. Develop a mathematical description of these processes and verify that it provides an accurate solution; and,
4. Interpret the results in relation to the observed physical reality.

Defining the modelling objective and developing a conceptual model are the most important steps in the modelling process. Again, this is where numerical modelling can be exceptionally useful, as the process forces the analyst to incorporate information on site geology and hydrogeology, laboratory information, and any other pertinent information (e.g., construction sequencing) into a conceptual model of the problem. The conceptual model must also be linked with the objectives of the modelling exercise.

Determining the appropriate theoretical model involves gaining an understanding of the underlying physics and the constitutive behavior governing material behavior. From the analysts' perspective, this is tantamount to ensuring that the formulation of the numerical model is representative of the physical process being explored. This understanding is manifest in a model's development through the definition of the boundary conditions and material properties. These components often change as the analyst iterates through the modelling process; refining the model as the understanding of the physical system evolves and additional field and laboratory data becomes available.

Eventually, the conceptual and theoretical models are committed to a mathematical solution. In a finite element analysis, the geometry of the problem domain is drawn, material properties are defined, and boundary conditions are applied to the domain. A verification of the solution is completed to ensure convergence, appropriate spatial and temporal discretization, and correct application of physics (perhaps via comparison with an analytical solution). A simple to complex mantra must be adopted, so that the analyst can be confident in the numerical solution.

Finally, the results are interpreted within the context of the physical reality. The most fundamental question that should always be asked is: are the results reasonable? Stated another way, interpretation of the results should be done with a skeptical mind-set. The results of the finite element analysis could be compared with field monitoring data and should always be interpreted in light of the information used to develop the conceptual and theoretical models.

A numerical model will likely evolve repeatedly over the course of the modelling process as the analyst is challenged by interpreting the results. Increasing complexity of the conceptual model may be required; however, speculating on high degrees of complexity in the absence of supporting observations is not just problematic, it makes the remaining parts of the process more difficult or impossible. The best numerical models include just enough complexity for the mathematical abstraction to reasonably approximate the physical reality.